Heliyon 9 (2023) e13390

Contents lists available at ScienceDirect

Heliyon

journal homepage: www.cell.com/heliyon

Research article

The use of a hybrid photovoltaic/thermal (PV/T) collector system as a sustainable energy-harvest instrument in urban technology

Singgih Dwi Prasetyo, Aditya Rio Prabowo *, Zainal Arifin **

ARTICLE INFO

Keywords:
PVT
Thermal collector
Solar energy
Nanofluid
Computational fluid dynamics

ABSTRACT

A solar cell is a converter that uses semiconductor material to convert photon energy packets. The electrons located in the material's crystalline structure can escape from the bonds between their atoms and generate electricity. Photovoltaic (PV) solar cells can work via diffuse radiation and have the highest efficiency among other types of solar cell generation. Photovoltaic Thermal Collector (PVT)-based active cooling technology makes it possible to increase the efficiency of PV solar cells and to generate thermal energy at the same time through the direct conversion of solar radiation. Therefore, this study modeled various riser configurations on PVT collectors to cool PV solar cells using water heat transfer fluids and nanofluids: TiO_2, SiO_2, and Al_2O_3. The mass flow rates were varied. An ANSYS models a simulation of the heat transfer phenomenon between the PV cell layer and the fluid. Only the heat transfer phenomenon generated from the natural convection of the PV cell layer is studied using steady-state thermal ANSYS with simulated controlled conditions. The radiation intensity of 1000 W/m^2 has the photovoltaic solar cells with the most negligible efficiency. The semicircular collector configuration with water at a mass flow rate of 0.5 kg/s demonstrated the highest electrical efficiency, achieving 11.98%.

1. Introduction

The use of sustainable, clean, and affordable energy is a prominent factor in economic and social development. Recently, solar energy has been widely used worldwide as a sustainable renewable energy source [1]. In Indonesia, solar energy is one of the types of renewable energy that the government actively develops because of its vast potential, having an energy utilization potential of 4.2–5.6 kWh/m^2 [2,3]. Using renewable, clean, and inexpensive energy sources like solar energy can help economic growth and social development [4]. In addition, solar energy does not produce pollutants, is sourced from nature, and is unlimited. Solar energy can be utilized by using solar cells via the photovoltaic process [5]. Solar cells are made of semiconductor material that changes the energy packet (photons). The electrons located in the crystal structure can escape from the bonds between its atoms to generate electricity. Three generations of solar cells have been developed so far. The first generation uses semiconductor materials that comprise poly-crystalline silicon (Si) or photovoltaic (PV) solar cells [6]. Second-generation solar cells form thin-film solar cells [7], and dye-sensitive solar cells, or DSSCs, represent third-generation solar cells [8].

PV solar cells are the ones that are the most widely used by the public to convert solar energy into electricity. This is because PV solar cells can work on diffuse radiation and have the highest efficiency among other generations of the solar cell. PV solar cells have

* Corresponding author.
** Corresponding author.
E-mail addresses: singgihdwipraset@student.uns.ac.id (S.D. Prasetyo), aditya@ft.uns.ac.id (A.R. Prabowo), zainal_arifin@staff.uns.ac.id (Z. Arifin).

https://doi.org/10.1016/j.heliyon.2023.e13390
Received 20 March 2022; Received in revised form 7 January 2023; Accepted 27 January 2023
Available online 1 February 2023

6–20% efficiency in converting solar radiation into electrical energy, depending on the climatic conditions where the solar cells are used [9]. The remaining unconverted solar radiation will turn into heat energy to increase the temperature of the PV solar cells. Increasing the temperature of a solar cell can decrease the performance of that PV solar cell. It is known that every 1 °C increase in temperature can reduce the efficiency of solar cells by ± 0.4–0.5% and can cause solar cells to short circuit [10]. Therefore, it is vital to lower the operating temperature of solar cells so that the PV modules can work effectively and protect the cells from heat damage.

Research on solar cell cooling technology could be a solution to the problem of energy scarcity. PV solar cells can be cooled via passive or active cooling. Passive cooling does not require external energy to cool the solar cells. It uses refrigerants from phase-changing materials and natural air conditioners, so less external power is needed. Passive cooling can lower the temperature of the solar cells by up to 292 K, increasing efficiency by 8.3% [11,12]. The use of active cooling can significantly reduce the temperature of the solar cell, and the efficiency is increased by 12%–14%, which is better than the efficiency achieved by passive cooling [13]. Active cooling uses external energy to move fluids and absorb heat. Active cooling can be achieved using nanofluids or water with a fan or pump [14].

Photovoltaic Thermal Collector (PVT)-based active cooling technology makes it possible to increase the efficiency of PV solar cells and generate other types of energy simultaneously through the direct conversion of solar radiation [15]. This cooling utilizes fluid flow in a pipe with a specific model attached to the bottom of the solar cell. The fluid can flow using energy from the water pump. It is known that the cooling fluid temperature continues to increase with time [16]. When the cooling fluid temperature increases, the ability to absorb heat will increase and cause the temperature of the solar cell to decrease, meaning that the performance and efficiency of the PV solar cell will also increase [17]. In addition, the hot fluid that is produced can be utilized and adapted for different uses. Nanoparticle-based nanofluids can increase the thermal conductivity, viscosity, density, and convective heat transfer coefficient. TiO_2, SiO_2, and Al_2O_3 are nanofluids that can be used as coolants. The use of nanofluids can increase efficiency by 2.6% and water use by 3% [18–20].

The use of PVT and the parameters of the shape of the collector configuration and flow rate increase PV performance because of the ease of heat transfer. The fluid flows into a collector made of aluminum. The direct flow configuration has a good heat transfer capability and an easy-to-fabricate configuration design [21]. Collectors with natural flow PVT have been successfully modeled, and heat transfer simulations have been carried out using the ANSYS Computational Fluid Dynamics (CFD) system [22]. The results of modeling and simulation on actual conditions at minimum costs [23,24]. The simulation results show that using a mass flow rate of 0.03 kg/s with a SiO_2 fluid with an intensity of 1000 W/m^2 produces the most significant electrical efficiency of 12.70% [25].

Meanwhile, Rosli et al., in 2018 also reported an increase in the electrical efficiency and an increase in the mass flow rate. The simulation results showed an electrical efficiency of 11.67% with a mass flow rate of 0.005 kg/s when water with a radiation intensity of 1000 W/m^2 was used [26]. In 2018, Hernando et al. reported differences in the cross-sectional shape of the riser configuration on the collector based on whether it was round or square. The different forms resulted in other PVT efficiencies, as shown in Fig. 1. The pipe diameter does not affect thermal efficiency, but doubling the number of riser tubes causes an absolute increase in the thermal efficiency of 1.5% or a relative increase of 2.3% [27,28].

Therefore, Eisavi et al. modeled various forms of riser configurations on PVT collectors to cool PV solar cells in their 2021 study using heat transfer fluids: water and TiO_2, SiO_2, and Al_2O_3 nanofluids, and varying mass flow rates. Modeling was done using the ANSYS coupling program as the simulation method. This simulation method provides accurate results due to the high flexibility of the riser configuration without having to spend much money. Three-dimensional PVT modeling aims to identify and compare the operating temperature of PVT solar cells with various treatments. Some researchers use the CFD approach to analyze multiple energy conversion systems to study heat transfer [29,30]. The heat transfer phenomenon between the PV cell layer and water was simulated and modeled using Fluent software. The heat transfer phenomenon derived from the natural convection of the PV cell layer was studied using a steady-state thermal device with simulated steady-state conditions. This simulation method can provide accurate results by providing a riser configuration with high flexibility without spending much money [31].

2. Literature review

2.1. Solar cells

One source of renewable energy that is available anywhere in the sun. The reaction between the fusion of hydrogen and helium results in electromagnetic radiation that can be emitted by the sun. The radiation that is emitted can be converted into energy.

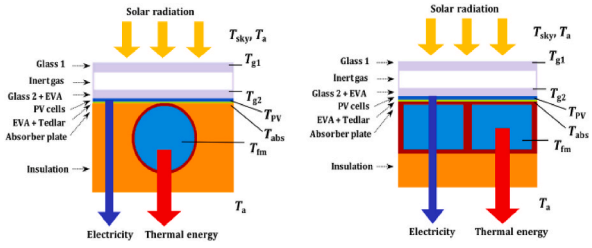

Fig. 1. Configuration of the PVT collector riser [27].

According to the World Radiation Center (WRC), the solar constant is 1367 W/m^2 [32]. The energy contained in solar radiation, known as solar energy, can be converted into electrical energy. About 53% of solar radiation comprises the infrared spectrum, with the electromagnetic waves being >700 nm [33]. The solar radiation spectrum converted into electrical energy with a silicon-type solar energy harvester is 23% [34]. Various types of solar cells can be used in everyday life. Each type of solar cell has advantages and disadvantages, both of which are shown in Table 1.

Photovoltaic solar cells are a solar energy harvesting technology that uses semiconductor materials with a photovoltaic effect to convert solar radiation into direct current electricity. Photovoltaic solar cell technology was originally invented by French physicist Alexander Becquerel, who successfully generated electricity directly from solar energy [35]. Over time, the photovoltaic solar cell industry became the fastest-growing energy industry. Photovoltaic solar cells have become widely used, especially in developed countries, to overcome the depletion of fossil energy. Photovoltaic cells using silicon materials still dominate the market due to their 14–17% efficiency and their service life of 25 years [36]. Developments are consistently carried out to improve system technology and reduce photovoltaic maintenance and installation costs, meaning that they are more affordable and available to the wider community.

2.2. Solar cell cooling

The increase in the heat transfer rate via convection and conduction is influenced by the convection coefficient of the substance, the cross-sectional area of the heated substance, the coefficient of thermal conductivity, and the temperature difference from where the object is heated to the specified place. Therefore, the heat absorption achieved in PV solar cells using the Photovoltaic Thermal Collector (PVT) cooling method depends on the design, operational, and climate parameters. Many designs have been considered to improve photoelectric performance, and for this purpose, PVT collectors have been proposed. Good thermal conductivity between the heat absorption unit and the photovoltaic module can increase the electrical and thermal efficiency [37].

A Photovoltaic Thermal Collector is an active cooling technology for photovoltaic solar cells. Collectors are installed behind the photovoltaic cells. Therefore, the cells are cooled by the heat transfer medium in the collector while also generating electricity. Refrigerants, water, nanofluids, air, or a combination of liquid and air can be used as the cooling liquid. The advantages of air cooling include increased overall efficiency and no economic limitations, and hot air can be used to heat buildings in the winter. However, the resulting efficiency is lower than water cooling [38]. Many studies have evaluated the factors that affect PVT performance in simulations or experiments. Parameters that can affect performance include design, operational, and climate parameters. Many designs have been considered to improve photoelectric performance, and for this purpose, PVT collectors have been proposed [39].

PVT solar cell collectors are the main functional element, as the sun-induced heat transfer that is collected by the photovoltaic laminate to the fluid. The flow design must allow for the heat from the solar cell to pass through the fluid. The best flow designs that have been reported are spiral designs. The direct flow pipe produces better efficiency, which is 64% compared to a single pass pipe [21]. The specific heat capacity of the collector should be of a low value to allow for fast reaction times according to different meteorological conditions (e.g., in the presence of fluctuating conditions) and to optimize the management of the available heat energy, even in low quantities. Its main properties are its thermal conductivity and specific heat capacity. PVT collectors are generally made of metal materials, such as copper, aluminum, or stainless steel. Researchers have conducted experiments on the type of aluminum pipe. Aluminum pipes do not experience erosion when water or nanofluids flow through them. The top of the collector allows for the perfect adhesion of the PV cell or laminate, thereby increasing the heat dissipation of the photovoltaic components [40]. Different types of plates differ according to their forming technique, which also determines the choice of material to be adopted and the configuration of the channel. The collector design can be in a roll bond, box, or trapezoid, as shown in Fig. 2.

2.3. Applications of photovoltaic thermal collector systems

There has been a great deal of research that has been conducted on PVT collectors over the last few decades. Hegazy et al. covered design development, numerical simulation, prototype design, testing, and test methods for collectors. This was achieved by comparing the performance of four commonly used PVT gas collector configurations. The numerical solution of the energy balance shows that the electrical and thermal efficiency for models II-IV is the same and higher than those for a model I and that the required pump power is the lowest for models III and t IV [42]. Research on improving PVT gas collectors by increasing heat extraction has also been carried

Table 1
Types of solar cells and their advantages and disadvantages [3].

Generation solar cells	Benefits	Disadvantages
Silicon solar cells	• High efficiency • Many are sold on the market	• Expensive • The complicated and complex fabrication process • Efficiency decreases at high temperatures
Film solar cells	• Cheaper than the first generation of solar cells	• Performance decreases over time • Poor stability • Lower efficiency than silicon solar cells
Dye-Sensitized Solar Cell (DSSC)	• The high solar absorption coefficient • Raw materials are easy to find • Easiest fabrication • Low cost compared to other types	• Use a liquid electrolyte for manufacturing, so it is volatile (low stability) • Not widely commercially available

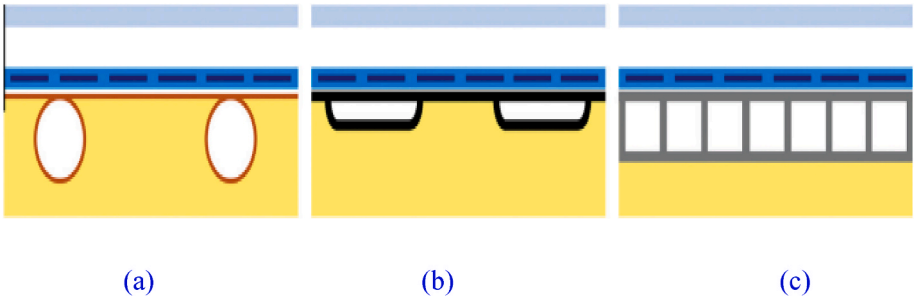

Fig. 2. Shape schematic for PVT collector riser (a) sheet and tube (b) roll bond (c) box channel [41].

out. The literature reports 30%, 28, and 25% for finned hanging metal panels and conventional air heaters [43]. Finned systems are beneficial for higher latitudes where more heat needs to be acquired during the winter, while PVT systems have metal suspensions. Some progress has been made in the research related to technological advances in the integration of PVT applications, as shown in Table 2.

Table 2
PVT applications [3].

Application	System	Benefits	Development
Building an integrated photovoltaic thermal collector	Active solar heating systems use collectors to channel working fluid attached to the walls or roof of the building. Transfer of radiant energy into electrical energy using PV solar cells and collector systems for storing solar energy in the required space [44].	Reduces fossil fuels by up to 30% [45].	Increased efficiency using phase change materials (PCM) for indoor thermal enhancement has been evaluated. PCM usage can be increased by 2.1%. The optimization effect of the collector design was studied by increasing the efficiency of PV solar cells by 23.7% [46].
Solar cell temperature-cooling control	Technology for converting solar energy through solar collectors to provide heating and cooling. The refrigeration cycle is widely applied for food processing, food preservation, chemical production, and environmental cooling applications [47].	Environmentally friendly and reduces emissions [48].	The development of collector types for heating absorption results in a primary energy savings of 50% when solar energy absorption cooling systems are used and 10–35% maximum electricity efficiency [49].
Water desalination	Desalination with solar energy is a common combination, and photovoltaic thermal collector desalination systems utilize waste heat from PV cells or generated electricity to remove salt from seawater [50].	Thermal water desalination with solar concentrators increases freshwater production by 57% [51].	Flat plate PVT systems have been widely applied, but these collectors can only reach low-range temperatures of 40–60 °C [52].
Solar drying	An effective method to inhibit the growth of microorganisms and avoid food contamination. Solar dryers have potential use in areas with high insolation and large amounts of sunshine [53].	Solar dryers can reduce the weight and volume of crop yields and can minimize packaging, storage, and transportation costs [53].	The precise design of solar dryers can meet the various drying requirements of plants and can improve energy efficiency. When the solar dryer is equipped with a PVT collector, it can simultaneously meet the drying and electricity consumption requirements. Additionally, it helps keep the farm protected. The air PVT collector's average thermal, electrical, and overall thermal efficiency can reach 26.88%, 11.26%, and 56.30%, respectively [44].
Active Solar PVT	Active solar operates with external energy support, and external energy is fed to the system basin; then, the water temperature in the basin increases with the integration of a flat plate collector [54].	Total drinking water productivity can be increased due to preheating the brine using flat plate collectors [55].	Developing a flat plate collector basin with an integrated active Solar PVT system results in thermal exergy and electrical exergy, and the overall thermal efficiency was 20.74%, 28.53%, and 69.06% [54].
PVT integrated into the vehicle	PVT technology with electric and hybrid vehicles can be used in two different modes. The first mode is installing a solar PVT station to recharge the hybrid electric vehicle, and the second is to integrate the PV panels with the vehicle directly. This solar-powered electric vehicle was designed to address the future crisis regarding non-renewable energy resources [56].	Reduces fuel oil and pollution because about 18% of the CO_2 emissions in industrialized countries come from the transportation sector [57].	Research with prototype solar hybrid vehicles developed from conventional cars with several electrical components such as in-wheel motors, photovoltaic panels, and Li-ion batteries installed [58]. In addition, a solar PVT station with an inductive power transfer method to recharge electric vehicles with a power capacity of 6.62 kW has been developed and was designed to restore four electric vehicles simultaneously [59].

2.4. Suitability and potential opportunities of photovoltaic thermal systems

Compared to other energy sources, there are many potential advantages to using solar energy with PVT technology: First, it has high performance, high reliability, and long service life. Second, it is a clean technology that can operate without using or producing toxic waste, such as radioactive materials. However, the disadvantages are obvious and cannot be ignored: the cooling effect is uneven, an innovative water absorption design is required, the efficiency is low, the payback period is long, and the return is not ideal [60]. The possibility of photovoltaic collectors being used as an energy source for this technology will also increase. Comparative analysis shows that the overall performance of photovoltaic thermal systems is better than systems with separate photovoltaic panels and solar thermal collectors to meet energy requirements. In addition, the integration of PV technology with electric, hybrid, and autonomous vehicles represents a green and sustainable step toward eliminating carbon in the transportation sector [61].

The application of PVT systems is highly dependent on climatic conditions. It is common for PVT systems to convert solar energy into electricity and heat. Still, additional energy input is also required to meet the energy supply requirements [62]. In addition, PVT systems provide both heat and electricity. Excessive energy can be wasted in geographic locations where the simultaneous use of both is not necessary. This problem can be solved by implementing an energy storage system. Therefore, it is required that the system be designed appropriately to effectively expand the PVT market. PVT technology combines the advantages of each unit into one system, providing hot water and electricity, and heat dissipation increase the efficiency of photovoltaic cells. It is expected to have great market expansion potential and help solve environmental problems. PVT can be applied using air or fluid, as shown in Table 3.

3. Materials and methods

The CFD method applied in this study was carried out using the ANSYS Fluent program [67]. This program can model convection heat transfer using the finite element method in a closed system, which means mass is constant. Steady-state modeling can be used to examine fluid flow in the collector model. This program can also simulate the solar radiation acting on solar cell models using the ANSYS Steady-State Thermal software. The research used the ANSYS 18.2 workbench software to determine fluid flow and heat transfer in the studied PVT. The heat transfer phenomenon between the PV cell layer and the fluid was modeled with ANSYS Fluent software.

In contrast, the steady condition ANSYS Steady-State Thermal software was used to simulate the heat transfer phenomenon derived from the natural convection of the PV cell layer. No solar radiation heat transfer simulations were carried out, and only different heat fluxes are considered in the PV cell layers. The geometric model of the CFD analysis was created using Solidworks 2018 software, and the meshing was completed using ANSYS meshing software [31].

The modeling carried out in the present research is influenced by the solar radiation applied to the surface of the PV solar cells so that only convection losses occur. In PV solar cells, fluid flows from the inlet to the outlet. The process results in increased PV efficiency and power—a schematic of the process is shown in Fig. 3.

Assumptions:

- The collector is perfectly isolated;
- Perfectly isolated collector;
- PV radiation loss is negligible;

Table 3
Types of PVT [3].

Type	Collector Design and Performance	Building Integration Applications
PVT–Air	The air-type design provides simple and economical cooling PV solar cells. The air can be heated to different temperatures through forced or natural flow. The design includes the alternative placement of the solar and thermal collector sections on the PV section. The resulting high-temperature air cools devices during summer and facilitates direct domestic hot water systems without additional heating devices. Simulation and experimental parametric studies yield advantages under mass flow conditions, with thermal efficiency reaching 80% [63].	Used on roofs of buildings with insulated walls on the inside with top and bottom ventilation openings to provide natural circulation. It can improve the room's thermal conditions and generate electricity. The indoor temperature increases by 278–280 K in the winter and maintains a PV solar cell efficiency of 10.4% [64].
PVT–Liquid	Energy performance of a PVT/w collector in which a c-Si solar cell (with or without a front cover) is immobilized on a polymer heat sink. The opposite surface is black (absorption coefficient for normal occurrence = 0.94), which allows it to function as a solar collector when rotated up and down. The square duct absorber is filled with ceramic particles. This increases the amount of heat transferred to the tap water. Analysis shows that existing solar cells reduce thermal absorption by about 10% of the incident radiation, while cover glass (if any) reduces optical efficiency by about 5%. Low-temperature applications are promising for hot water systems [65].	The roof-mounted BiPVT/w system is integrated into a standing wall or slab roof, where a duct is added to the body for coolant flow. Their modified Hottel–Whillier model was validated on a steady-state outdoor thermal test rig. The results show that key design parameters such as fin efficiency, laminate requirements, and thermal conductivity between the photovoltaic module and the supporting structure significantly affect the electrical and thermal efficiency. They also recommend limiting expensive materials, such as pre-coated steel instead of copper or aluminum, for heat absorption, as this does not significantly reduce efficiency. A rooftop model solar power plant is recommended for this system directly [66].

- There is no energy generator in the system;
- Fluid flow is steady-state;
- Convection loss only takes place in PV, and all heat is transferred in the fluid;
- Fluid flow is uniform;
- The ambient temperature around the system is constant;
- The thermophysical parameters of each solid layer of the solar device are considered consistent.

Factors affecting heat transfer:

- Thermal properties of fluid heat transfer: convection coefficient (h), thermal conductivity (k), and specific heat (c);
- Kinematic properties of fluid heat transfer (velocity and viscosity);
- Collector flow design (direct flow);
- Collector cross-sectional area (rectangle, semicircle, triangle);
- Type of contact of the collector with PV cell (contact area);
- Type of flow (turbulent).

The material modeled in this study is a photovoltaic solar cell module measuring 660 × 540 × 4.33 mm and has a temperature coefficient of −0.4%/K. The PV design structure refers to the geometric design [68]. The layout and specifications of the solar cells are shown in Table 4. In comparison, the design of the thermal collector in the form of direct flow refers to the research presented in Ref. [69].

All of the PV layers were modeled by varying the configuration of the riser collector, fluid input, and flow rate. The collector risers had rectangular, triangular, and semicircular configurations. Water and TiO_2, SiO_2, and Al_2O_3 nanofluids were the flowing fluids used. These nanofluids have good thermal conductivity, density, and viscosity compared to other nanofluids [71]. Other studies reported combined mass flow rates of 0.5, 0.05, and 0.005 kg/s. The fluid characteristics are described in Table 5.

The collector design used in this study was adapted from Refs. [25,26,69]. The collector is in direct flow and has input dimensions of 15 × 30 mm. In this research, we modified the shape of the collector design, namely rectangle (PP), triangle (S), and semicircle (SL). The thickness of the pipe in the simulation is considered to be 0 m because it is fragile, and aluminum was used as the collector material, as seen in Fig. 4.

3.1. Basic model

Basic models were developed using photovoltaic (PV) solar cells designed based on the research reported by Ref. [73]. The PV solar cells were 660 × 540 × 4.33 mm in size. The characteristics of the PV coating can be seen in Table. The collector has a basic design comprising a 660 × 540 × 15 mm beam size. Aluminum material with a fluid input of 1 m/s was used in the collector.

The basic models were simulated with ANSYS Fluent and Steady-State Thermal software. The atmospheric temperature was 298 K. The convection heat transfer coefficient (h) was 10 W/m^2K. The heat flux was only applied to the top surface of the PV solar cells was 800 W/m^2. Meshing was carried out adaptively with the "fine" classification. The nodes and elements in the PV solar cell mesh were 85,625 and 11,880, and there was an average mesh metric skewness of 1.31 E−8. After all of the boundary conditions were given, the PV solar cell temperature without cooling could be obtained. The results show that the PV solar cell temperature range was 298.15–376.6 K.

ANSYS Fluent software was used to simulate the PVP solar cell collector. Water is used in the collector. The Reynolds number is used to determine the type of flow in the collector, as Equations (1) and (2). The velocity used to represent the fluid input is 1 m/s [31].

$$Re = \frac{\rho V D}{\mu} \tag{1}$$

Here,

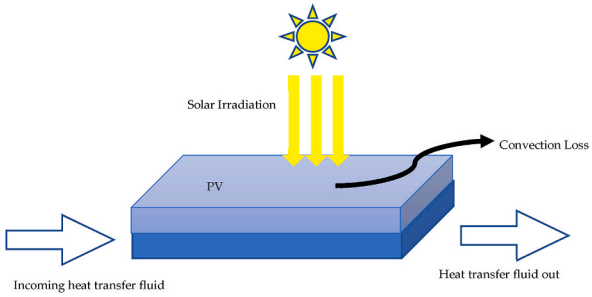

Fig. 3. PVT model schematic.

Table 4
Specifications of PV cell layer [70].

Layers	Density (kg/m^3)	Specific heat capacity (J/kgK)	Thermal conductivity (W/mK)	Thickness (mm)
Glass	2450	790	0.7	3.2
EVA	960	2090	0.311	0.5
PV cell	2330	677	130	0.21
EVA	960	2090	0.311	0.5
PDF	1200	1250	0.15	0.3

Table 5
Fluid characteristics [71,72].

Type	Thermal Conductivity (W/mK)	Density (kg/m^3)	Viscosity	Specific Heat (J/kgK)
Water	0.6	998.2	0.00899	4182
TiO_2	8.4	4100	31.2	697
SiO_2	13.0	5600	129.2	667
Al_2O_3	36.0	3600	28.2	773

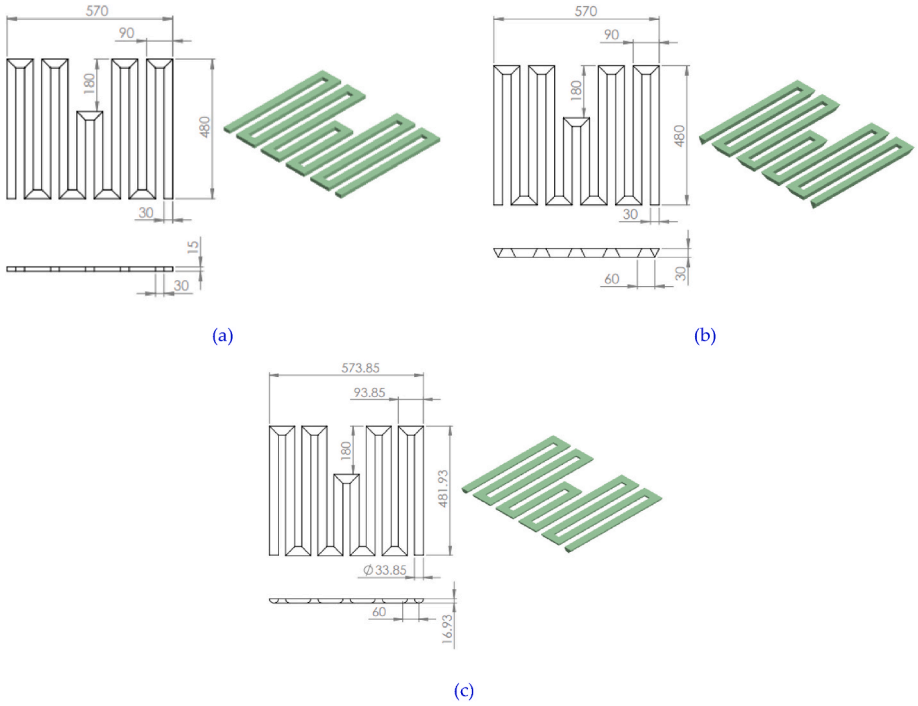

Fig. 4. Collector riser shape design (in mm): (a) rectangle, (b) triangle, (c) semicircle.

$$D = \frac{4A}{P} \tag{2}$$

$$D = \frac{4x(0.54x0.015)}{2x(0.54 + 0.015)} = 0.029189189\ m$$

- Density of water (ρ) = 998.2 kg/m^3;
- Dynamic viscosity (μ) = 0.001003 N/m^3.

Then, using Equation (1) produces

$$Re = \frac{998.2x1x0.029189189}{0.001003} = 29049.50$$

It is known that the Reynolds number is 29049.50, so it can be said that the water flow in the collector is turbulent. The k-ϵ model was used to simulate the turbulent flow [31,68]. A water fluid input temperature of 298.15 K was used for the simulation. The turbulence equation was used to model the effects of turbulence mathematically. The m model was used. The Re-Normalization Group (RNG) k-ε model is recommended for modeling the flow in air vents [68,74].

Equation (3) for the turbulent kinetic energy (k) is as follows:

$$\frac{\partial}{\partial t}(\rho k)+\frac{\partial}{\partial x_i}(\rho k u_i)=\frac{\partial}{\partial x_j}\left[\left(\mu+\frac{\mu_t}{\sigma_k}\right)\frac{\partial k}{\partial x_j}\right]+P_k-\rho\varepsilon \tag{3}$$

Equation (4) for the turbulent energy dissipation rate (ε) based on Equation (5) is as follows:

$$\frac{\partial}{\partial t}(\rho \varepsilon)+\frac{\partial}{\partial x_i}(\rho \varepsilon u_i)=\frac{\partial}{\partial x_j}\left[\left(\mu+\frac{\mu_t}{\sigma_\varepsilon}\right)\frac{\partial \varepsilon}{\partial x_j}\right]+C_{1\varepsilon}\frac{\varepsilon}{k}P_k-C_{2\varepsilon}^{*}\rho\frac{\varepsilon^2}{k} \tag{4}$$

where

$$C_{2\varepsilon}^{*}=C_{2\varepsilon}+\frac{C_\mu\eta^3\left(1-\frac{\eta}{\eta_0}\right)}{1+\beta\eta^3};\eta=\frac{Sk}{\varepsilon};S=\left(2S_{ij}S_{ij}\right)^{1/2} \tag{5}$$

Simulations of the water collector were carried out using ANSYS Fluent software coupled with ANSYS Steady-State Thermal software. Simulations were carried out to determine the temperature of the PV solar cells and the water collectors. The simulation results show a change in PV temperature when cooling without a water collector cooler. Temperature results obtained when water collector cooling was carried out on the basic model produced a range of 298.15–298.42 K. It is known that there are no significant temperature changes taking place at the collector between the inlet and outlet. The resulting temperature in the water collector is in the range of 298.38–298.41 K.

Based on the temperature generated in the simulation, it is known that the temperature decreases when water collectors are used to cooling PV solar cells. The decrease in temperature that occurs can also increase the efficiency of the PV solar cells. As such, it can be classified into.

- Tc (maximum PV temperature without cooling) = 376.60 K;
- Tc (maximum PV temperature with cooling) = 298.42 K;
- Electrical efficiency without cooling = 7.76%;
- Electrical efficiency with cooler = 11.99%;
- Relative increase in electrical efficiency = 54.38%.

The thermal energy output of the system is close to zero because there is no temperature rise in the outlet water that is released from the thermal collector system. Sa such, new modifications are needed in cases where electrical and thermal power are obtained simultaneously.

3.2. Research validation

Validation was carried out to prove that the simulation results were valid. This was carried out by equating the temperature distribution and PVT efficiency results through the collector model with the study results [26]. If the average temperature value in the photovoltaic cell was within 10% of the value stated in other published studies, then the design was declared valid. The error standard was set based on incorrect use in typical PVT simulations.

The model has a serpentine shape, is made of aluminum and mounted on the back of the layer, and has solar cell properties. The layers of solar cells are attached to various materials to form one piece, as shown in Fig. 5 (a). The dimensions of the solar cell layer to

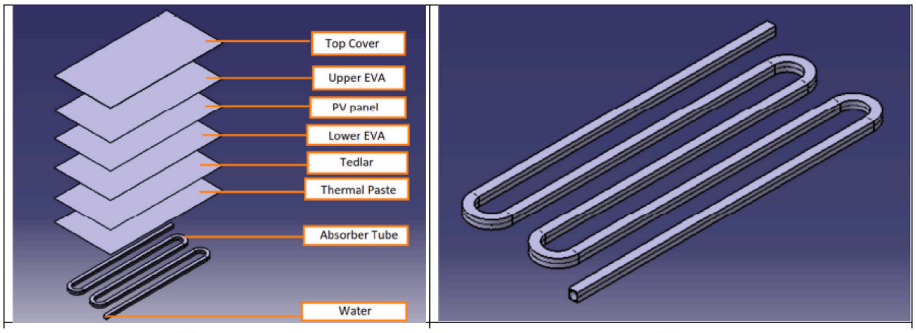

Fig. 5. (a) PV solar cell layer and (b) collector [26].

be validated were 1000 × 500 × 4.25 mm. As shown in Fig. 5 (b), the collector has dimensions of 26 × 26 mm and is 1800 mm in length. The validation model used a flow rate variation of 0.005 kg/s with water at a radiation intensity of 1000 W/m^2. The fluid and environmental input temperature were 298.15 K. The geometry of the collector and PV solar cells has the same specifications as the geometry used for the validation of this study. Validation was conducted via simulations conducted according to the basic model [26].

The validation results determined the average temperature of the PV cells, which is illustrated by the temperature contour shown in Fig. 6 (a). The literature reports the PV cell temperature ranges from 300.10 to 307.10 K. Meanwhile, the reported electrical and thermal efficiencies are 11.67 and 22.62%, respectively [26]. The PV cell temperature range obtained via the validation simulation was from 298.15 to 306.15 K, as seen in Fig. 6 (b). The electrical and thermal efficiency generated in the validation simulation were 11.93 and 24.40%, respectively. The resulting errors were 2% and 8%, meaning the simulation configuration can be declared valid [12,31,38,68].

3.3. Meshing strategy

Meshing was carried out using the default configuration for the mesh application. The smoothing level of the mesh became smooth. The mesh model used in the simulation process is in the form of curvature. Apart from that, there were no changes to the default configuration. A tetrahedral geometry was formed in the mesh, while the PV geometry uses a mesh by default. Mesh independence testing was carried out to determine the most suitable mesh size for a particular geometry [26,28,36]. During the PVT treatment, the mesh test was carried out with a fluid mass flow rate of 0.0005 kg/s at a radiation intensity of 1000 W/m^2. The input and ambient temperatures were 298.15 K. Mesh variations were carried out by changing the treatment of the mesh element, which was applied in the range from 6 to 24 mm. The mesh test was carried out to determine the average final temperature on the PV after being cooled with a collector. In Fig. 7, it is known that the use of mesh elements that range from 12 to 16 mm achieves more stable results, and the required simulation time is not too long. Therefore, this study used an element size of 14 mm for the mesh simulations.

Mesh elements 12–16 mm in size are more stable, allowing them to capture the flow and heat transfer phenomena that occur in the area around the collector more accurately. There were 12,375 and 207,746 mesh elements that were 14 mm in size on the PV and collector, respectively. The resulting mesh shapes are shown in Fig. 8. The quality of the mesh for each geometry is shown in Table 6.

3.4. Boundary conditions

ANSYS Fluent software uses steady-state simulations and the k-ε Re-Normalization Group (RNG) turbulence model. The fluid mass flow rates were varied by 0.5, 0.05, and 0.005 kg/s, with a temperature of 298.15, turbulence intensity of 5%, and hydraulic diameter of 0.02 m. The COUPLED Green Gauss Cell-Based solution method was used. The convergence criteria set were E−6 for energy and E−4 for pressure, velocity, and continuity equations.

Meanwhile, the ANSYS Steady-State Thermal software simulations were carried out under steady-state conditions. A heat flux module modeled solar radiation values of 600, 800, and 1000 W/m^2. Solar radiation is arranged so that the solar energy hits the surface of the PV cell, while the other domain surfaces are affected by convection losses. Only small amounts of convection heat transfer are assumed to occur at the surface of the PV cell when the convection coefficient is 10 W/m^{2}K. The fluid-solid interface is used on the top surface of the PV [68].

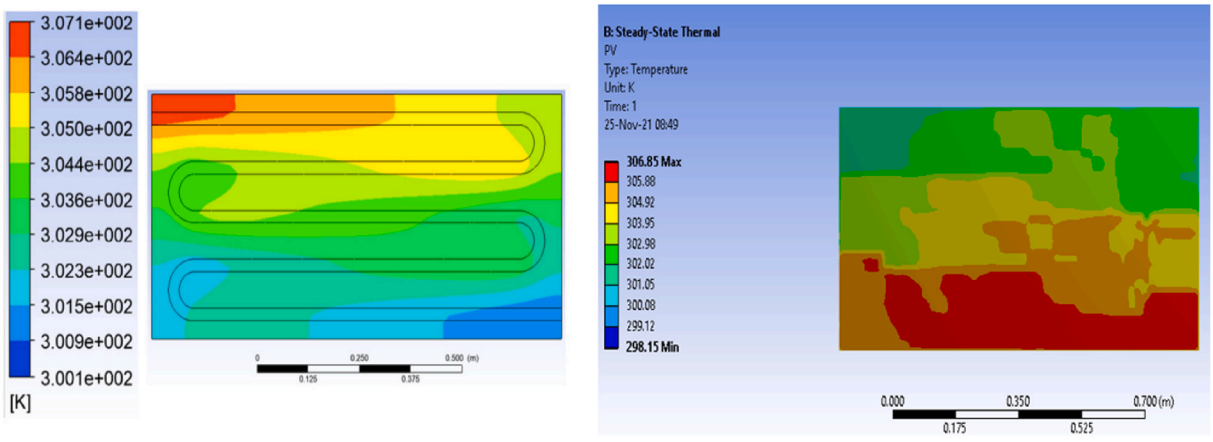

Fig. 6. Results of the PV surface contour simulation results from (a) reference [26] and (b) the present research.

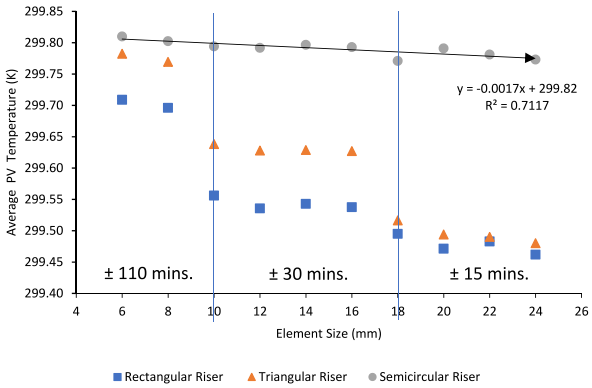

Fig. 7. Mesh independence in the present research.

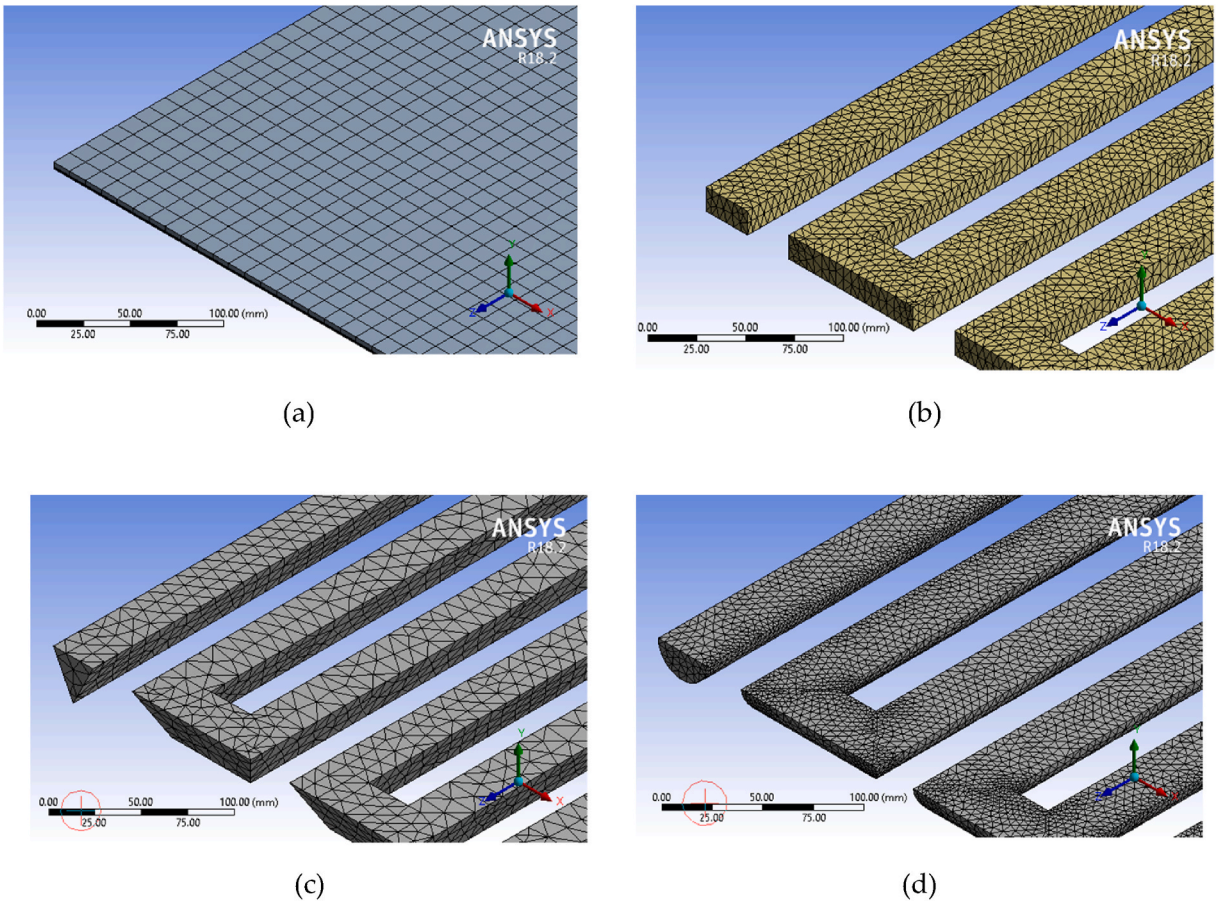

Fig. 8. Element mesh 14 mm: (a) PV, (b) rectangular riser, (c) triangular riser, (d) semicircular riser.

Table 6
Quality of the mesh design element for a 14 mm mesh geometry.

Average mesh metric 14 mm	Skewness	
	Collector	PV (E−8)
riser Rectangle	0.27	7.82
riser Triangle	0.34	8.04
riser Semicircle	0.27	8.04

3.5. Performance analysis

The value of the electrical efficiency of photovoltaic (PV) cells is inversely proportional to the significant increase in the cell's operating temperature during the absorption of solar radiation. Electrical efficiency can be expressed using the following Equation (6):

$$\eta_{el} = \eta_{ref}\left[1 - \beta_{ref}\left(T_c - T_{ref}\right)\right] \tag{6}$$

Where η_{ref} represents the reference efficiency of PV solar cells, β_{ref} represents the temperature coefficient of PV solar cells, and T_{ref} represents the initial PV reference temperature. When T_{ref} is 298 K, ref and ref are 0.12 and 0.0045/K for silicon-based PV solar cells. CFD simulations were used to determine the final maximum PV temperature to calculate the efficiency using this equation against the η_{ref}, β_{ref}, and T_{ref} previously determined [26]. The thermal efficiency can be determined using the following Equations (7) and (8):

$$\eta_{th} = \frac{Useful\ energy\ gain}{total\ solar\ irradiance\ received} \tag{7}$$

$$\eta_{th} = \frac{mc_p\left(\left(T_o - T_i\right)\right.}{IA} \tag{8}$$

where m is the mass flow rate, c_p is the specific heat capacity of the heat transfer fluid, and T_o is the output temperature generated during the CFD simulations on the fluid. T_i is the initial temperature of the fluid introduced to the collector. I represent the intensity of the sunlight, and A is the cross-sectional area of the collector. Total efficiency is obtained from thermal efficiency and electrical efficiency as Equation (9) [26].

$$\eta_{total} = \eta_{el} + \eta_{th} \tag{9}$$

Based on the statistical value to be reported, An ANOVA analysis was carried out to determine the homogeneity. The research was conducted using a significant value of 0.05. The hypothesis was determined based on the formulation of the existing problem. The null hypothesis (H01) for the riser configuration states that the shape of the PVT collector riser configuration does not affect the efficiency of photovoltaic solar cells. Null hypothesis two (H02), which discusses the use of nanofluids as a working fluid, states that the working fluid does not affect the efficiency of photovoltaic solar cells. Null hypothesis three (H03), which discusses the fluid mass flow rate, states that the mass flow rate does not affect the efficiency of photovoltaic solar cells. The null hypothesis can be accepted if the *P*-value is more than the significance value [75]. On the other hand, Fig. 9 is a hypothetical scheme of the research activities carried out in the present research.

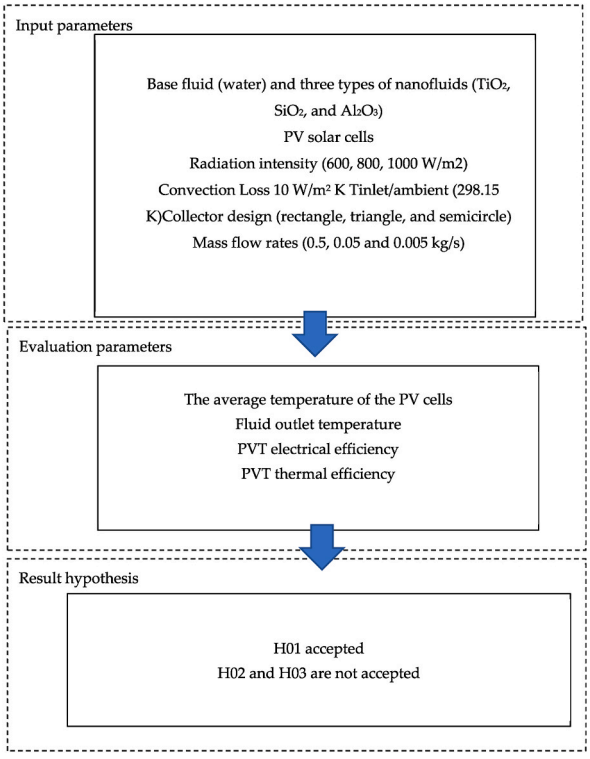

Fig. 9. Hypothesis schematic.

4. Results and discussion

Basic modeling and simulations were successfully conducted to determine the parameters affecting thermal collector systems. Design factors in the form of the riser collector configuration, fluid mass flow rate, working fluid, and radiation intensity should be considered when optimizing the performance of photovoltaic (PV) solar cells. Optimization was simulated using ANSYS Fluent and Steady-State Thermal 18.2. This chapter discusses the results found after the optimized design simulations. After the CFD simulation of the Photovoltaic Thermal Collector (PVT) system using the complete ANSYS software for all factors, all energy interactions and PVT efficiency (electric and thermal) were calculated. Based on these results, the influence of each design factor can be seen in the results of the ANOVA analysis.

4.1. Photovoltaic solar cell temperature distribution in thermal collector systems

The performance of PV solar cells is influenced by the temperature of the solar cells when converting photon energy. Photon energy conversion occurs when solar cells absorb the solar energy obtained from solar radiation. The excess heat can be better transferred to the surrounding fluid using a photovoltaic thermal collector [76]. Based on the basic model using photovoltaic thermal collectors, there is a relative increase in electrical efficiency. Collectors with direct flow models can be used to produce thermal energy simultaneously. The heating temperature is generated based on the intensity of the radiation that is produced [21,77].

Fig. 10 shows the maximum temperature simulation results in PV solar cells. Simulations vary based on the type of fluid used and the radiation intensity, with other factors being maintained when thermal collectors with a rectangular riser configuration are used. Using a fluid mass flow rate of 0.05 kg/s produces an increasing temperature trend as the intensity of the solar radiation increases. The use of solar radiation intensity of 1000 W/m^2 produces the highest maximum temperature for each type of fluid used. When Al_2O_3-based fluids were used, they produced a temperature of 307.97 K. The heat transfer to the collector fluid resulted in a high maximum temperature at the collector outlet. The temperature of Al_2O_3-based fluid at the outlet was 307.971 K.

Fig. 11 (a) shows the temperature distribution contour on the PV surface after the photovoltaic thermal collector system had been cooled using Al_2O_3-based fluid at a radiation intensity of 1000 W/m^2 and a fluid mass flow rate of 0.05 kg/s. However, the maximum temperature distribution is still wide on several sides towards the collector outlet, shown by the red contour. Fig. 11 (b) shows the temperature distribution on the collector fluid wall. The thermal collector for Al_2O_3 fluid is located below and attached to the PV solar cell, resulting in the contour being similar to the PV contour in shape and color. In contrast to the basic collector model, the direct flow collector system produces a thermal fluid. The fluid produced in Al_2O_3 in the cooling system reached 307.97 K. The fluid collector plays a role in the fluid flowing through the collector, helping to carry out heat transfer in PV solar cells [78].

Using a photovoltaic thermal collector system in photovoltaic solar cells increases the rate of heat transfer from the panel to the

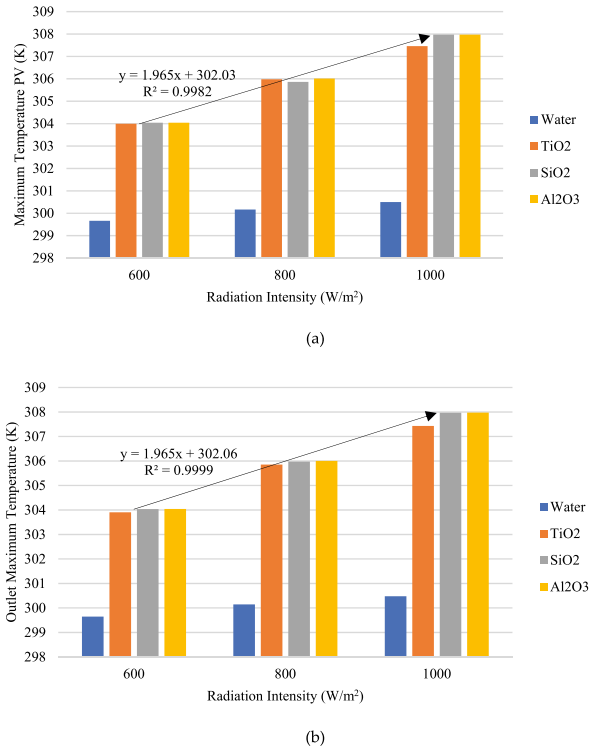

Fig. 10. Graph of the radiation intensity effects on the maximum temperature: (a) PV and (b) at the collector outlet.

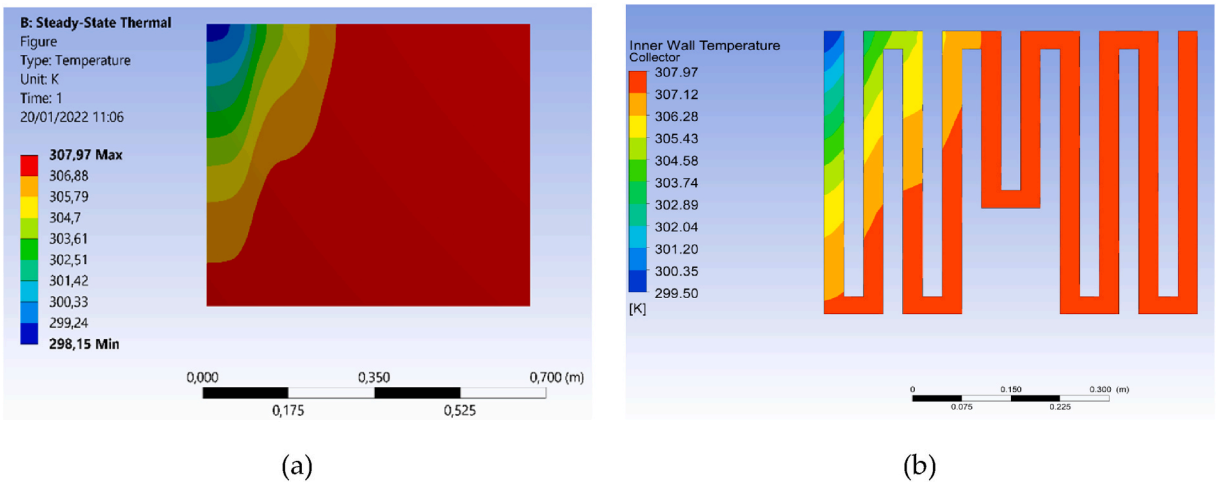

Fig. 11. Contours of the (a) PV and (b) Al_2O_3 thermal collector fluid with a radiation intensity of 1000 W/m$^{2.}$

fluid in the collector. When a refrigeration unit is installed at the rear of the solar cell, the heat transfer area increases according to the surface area of the refrigeration unit that is in contact with the collector fluid. Increasing the heat transfer area will increase the rate of convection heat transfer from the photovoltaic solar cells to the collector fluid and reduce the solar cells' operating temperature [79]. Cooling down the fluid at the highest radiation intensity of 1000 W/m^2 to reduce the working temperature and increase solar cell performance.

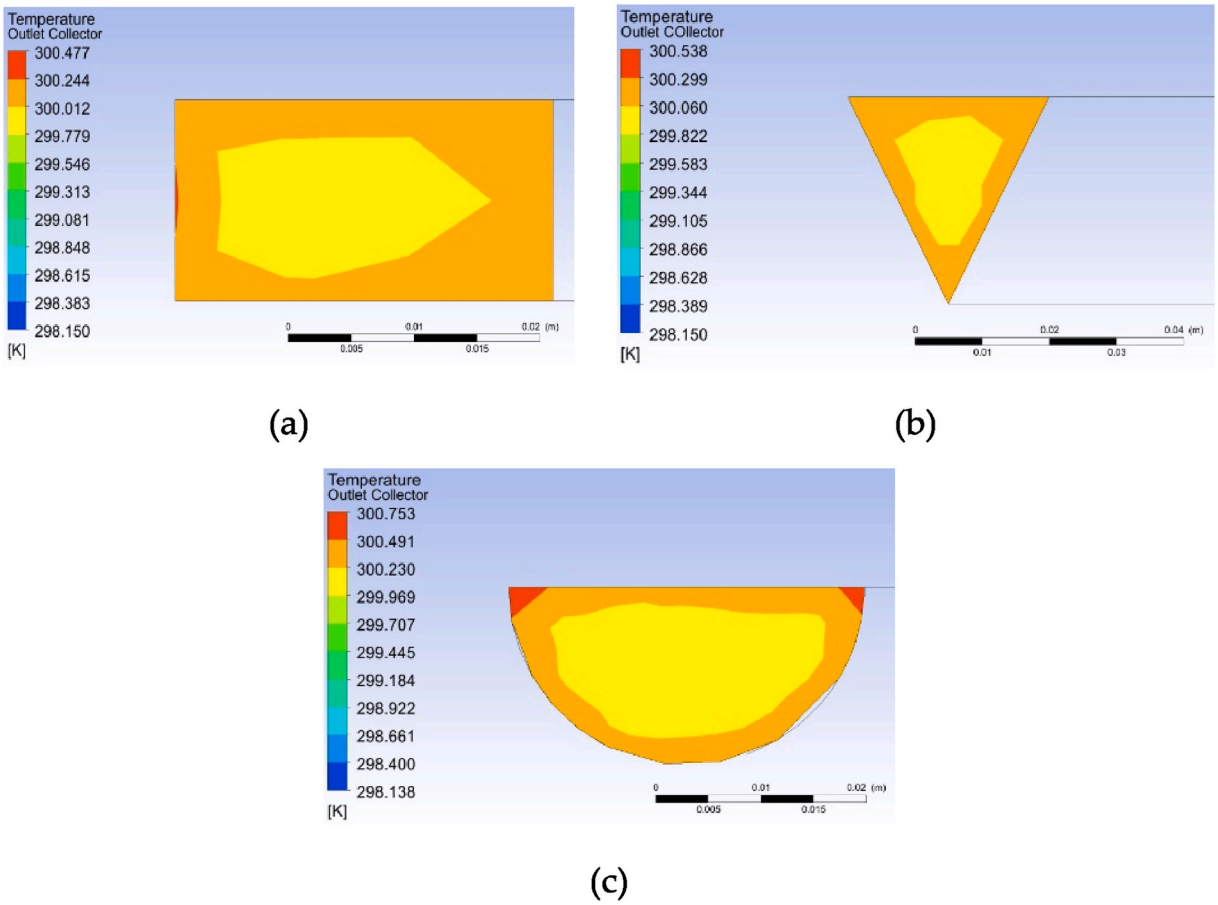

Fig. 12. Temperature contour of collector outlet when water is used in each riser configuration shape: (a) rectangle, (b) triangle, (c) semicircle.

4.2. Temperature distribution of photovoltaic solar cells in -thermal collector systems with different riser collector configuration shapes and fluid types

The collector is the main functional element in photovoltaic collectors because it transfers the solar energy collected by photovoltaic solar cells into the working fluid. The main properties required for the collector are thermal conductivity and specific heat [80]. Aluminum is more affordable and easier to find. In addition, it allows for perfect bonding between photovoltaic laminates or laminates, thereby increasing the heat transfer of photovoltaic solar cells [79,81]. The use of collectors with direct flow designs is easy to manufacture and assemble in photovoltaic thermal collector systems. The direct flow model provides a more continuous flow and less resistance, minimizing bending at every corner [82].

Different riser configuration shapes can be used, namely rectangles, triangles, and semicircles. The riser configuration has the same cross-sectional area value, regardless of the shape. As such, each shape has the same hydraulic value. The hydraulic value plays a vital role in facilitating the fluid flow rate, which affects the flow turbulence value. It can be seen that the same hydraulic value does not have much effect on the collector outlet temperature, even when different riser configuration shapes, namely rectangular, triangular, and semicircular. The shape of the riser configuration has the same cross-sectional area value. As such, each shape has the same hydraulic value. The hydraulic value plays a vital role in facilitating the fluid flow rate, which affects the flow turbulence value [83]. It can be seen that this does not have much effect on the collector outlet temperature when the hydraulic value is the same, as seen in Fig. 12 and Table 7.

As seen in Fig. 12 (a), the heat transfer contour on the collector is better than the other designs when the radiation intensity is 1000 W/m2 and when the mass fluid flow rate is 0.05 kg/s. More orange color contours indicate that the working fluid can absorb and transfer heat from the PV solar cells. Because the cross-sectional area of the PV has the same area, the collector side has a vital role in the collector's fluid flow process. Fluids with incompressible properties adapt to the shape of the container, indicating that the use of a rectangular riser configuration results in a more flexible cavity shape for the working fluid to transfer heat through [27]. As seen in Table 7, using Al_2O_3-based working fluid results in a higher collector outlet temperature value of 307.979 K in a semicircular collector. The lowest outlet temperature when water is used in a rectangular collector is 304.477 K.

The value of temperature difference at the collector outlet compared to at the collector inlet results in heat transfer at the temperature of the PV solar cell. The different collector riser configuration shapes result in drops in the maximum PV temperature. The value of the PV temperature is close to the value of the collector outlet temperature. As seen in Fig. 13, the difference in the riser configuration shows a temperature change trend but does not differ specifically. The lowest maximum PV temperature when water is used is 300.50 K. The fluid greatly influences the heat transfer process in PV solar cells [84]. In comparison, the shape of the riser collector configuration does not significantly affect the heat transfer process.

Fig. 14 shows the surface temperature contour of PV solar cells and collectors with different riser collector configurations and when water is used. The contours vary in color, and not much difference can be observed, regardless of the shape of the riser configuration used. Red contours are prominent on the PV surface. Meanwhile, for the collectors, dark blue is dominant. This shows a combination of heat transfer phenomena in the photovoltaic thermal collector system. Regardless of the various conditions maintained, water has a better retaining effect and heat transfer when used as the working fluid. It has a smaller thermal conductivity and density value.

When Al_2O_3 fluid was used when a semicircular shape was used for the riser collector configuration, the PV and collector surface contour looked similar to when water was used as the fluid, as shown in Fig. 15 (a) and (b); the contours vary in color, with red being dominant on the PV and collector surfaces. However, the use of Al_2O_3 fluid is higher than water by 307.64 K. Heat transfer in the working fluid is uniform, covering the entire cross-sectional surface, as shown in Fig. 15 (c). This is because the density value of the Al_2O_3 fluid is very high, so it has more time to convert heat [18].

There was a smaller lower temperature drop when water was used than when a nanofluid was used. The research presented here uses pure nanofluids with very high thermal conductivity values and low specific heat. This allows for faster heat transfer. However, the fluid flow is slow and retains heat [85]. Therefore, the maximum temperature value of the PV solar cells and the fluid is higher. The maximum PV temperature and the highest collector outlet when Al_2O_3 fluid was used were 307.98, and 307.979 K. Temperature changes will affect the performance of PV solar cells.

Table 7
Collector outlet temperature results for each riser configuration shape.

Collector Riser Configuration Form	Fluid	Temperature (K)
Rectangle	Water	300.477
	TiO_2	307.431
	SiO_2	307.968
	Al_2O_3	307.971
Triangle	Water	300.538
	TiO_2	307.849
	SiO_2	307.965
	Al_2O_3	307.976
Semicircle	Water	300.753
	TiO_2	307.951
	SiO_2	307.967
	Al_2O_3	307.979

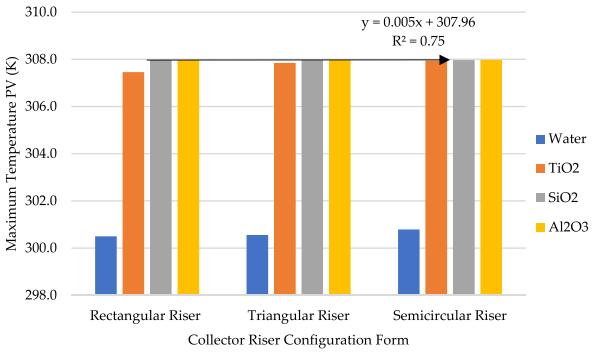

Fig. 13. Effect of the shape of the collector riser configuration riser on maximum temperature PV.

4.3. Photovoltaic solar cell temperature distribution in thermal collector systems with different fluid mass flow rates

The mass flow rate of the fluid was investigated in a photovoltaic thermal collector system to determine the temperature drop in photovoltaic solar cells. The fluid flow that passes through the collector transfers heat, affecting the electrical and thermal efficiency [86]. In this analysis, the mass flow rates used were 0.5, 0.05, and 0.005 kg/s, and 1000 W/m^2 was used as the radiation intensity. The effect of the fluid mass flow rate with the shape of the collector and the type of fluid on the temperature is shown in Fig. 16. The simulation results show that the lowest temperature was achieved using a mass flow rate of 0.5 kg/s. Using water at a fluid mass flow rate of 0.5 kg/s with a semicircular riser collector configuration resulted in the lowest maximum PV temperature of 298.56 K. As shown in the trend generated in the graph, a decrease in temperature occurs when the fluid mass flow rate increases.

A decrease can be observed in the differences in the temperature contours. In Fig. 17, there are variations in the color contours produced and scattered because of the direct flow direction. The red contour indicates high temperatures, while the blue indicates low temperatures. Using a fluid mass flow rate of 0.5 kg/s results in a blue contour that is more evenly distributed on the collector and the PV surface. It has a more dominant green contour. It seems as though a temperature distribution with fewer red contours than the others can be observed in Fig. 17 (c). This shows that better and more thorough heat transfer to the collector fluid occurred in the PV solar cells.

The absorption of heat transfer generates thermal fluid at the collector outlet. The maximum fluid temperature difference occurs at the outlet compared to the inlet. At the PV maximum temperature, the collector outlet with a semicircular shape has the lowest temperature when a mass flow rate of 0.5 kg/s is used. The lowest temperature produced is 298.540 K. The highest temperature is 307.998 K was achieved with a collector with a semicircular riser collector configuration and water with a mass flow rate of 0.005 kg/s, as seen in Table 8. The fluid distribution causes the temperature difference at the outlet of the collector at a specific mass flow rate.

Based on the fluid mass flow rate differences, there are also differences in the temperature distribution at the collector outlet. In Fig. 18, the temperature distribution varies, indicated by different colored contours. Using a mass flow rate of 0.005 kg/s, even an orange contour can be observed, indicating that the heat transfer to the fluid will be slower when the mass flow rate is slow, and the temperature will be maintained. This is because more time is required to change the fluid to transfer heat from the PV cell to the collector fluid. On the other hand, a mass flow rate of 0.5 kg/s produces a more varied temperature distribution contour. The green contour is yellow, which indicates a low collector outlet temperature. This is due to the faster heat transfer. This is because the working fluid transfers heat relatively quickly and because the working fluid that flows through it is renewed faster. Therefore, the fluid mass flow rate is strongly supported by the density value. Lower density values can accelerate the flow rate and avoid friction in the collector [87].

4.4. Photovoltaic solar cell efficiency in a thermal collector system

Using a photovoltaic thermal collector system reduces the maximum PV temperature. The maximum PV temperature was obtained from the simulation process coupled with the steady-state thermal model on the PV and the fluent model on the collector. The photovoltaic thermal collector system was used with a radiation intensity of 1000 W/m^2, which was achieved by varying the fluid type at a flow rate of 0.05 kg/s. The electrical efficiency of a photovoltaic thermal collector system is calculated by applying the same analysis if an electrical efficiency analysis was being carried out on a system without a photovoltaic thermal collector system. Using a photovoltaic thermal collector system has the advantage of allowing the thermal efficiency to be calculated.

Without a photovoltaic thermal collector system, the electrical efficiency has a lower value than the electrical efficiency when calculated for a photovoltaic thermal collector system. The highest electrical efficiency was determined at a radiation intensity of 600 W/m^2 and with 11.92% water. The lowest efficiency was determined at a radiation intensity of 1000 W/m^2 with 11.47% Al_2O_3 fluid, as shown in Fig. 19. The increase in electrical efficiency is caused by a decrease in the temperature of the PV solar cells. The heat transfer causes the reduction in temperature in the solar cell to the fluid contained in the photovoltaic thermal collector system. This causes the fluid temperature to increase [76].

The increasing fluid temperature in the photovoltaic thermal collector system enables that fluid to be used as a thermal fluid. The

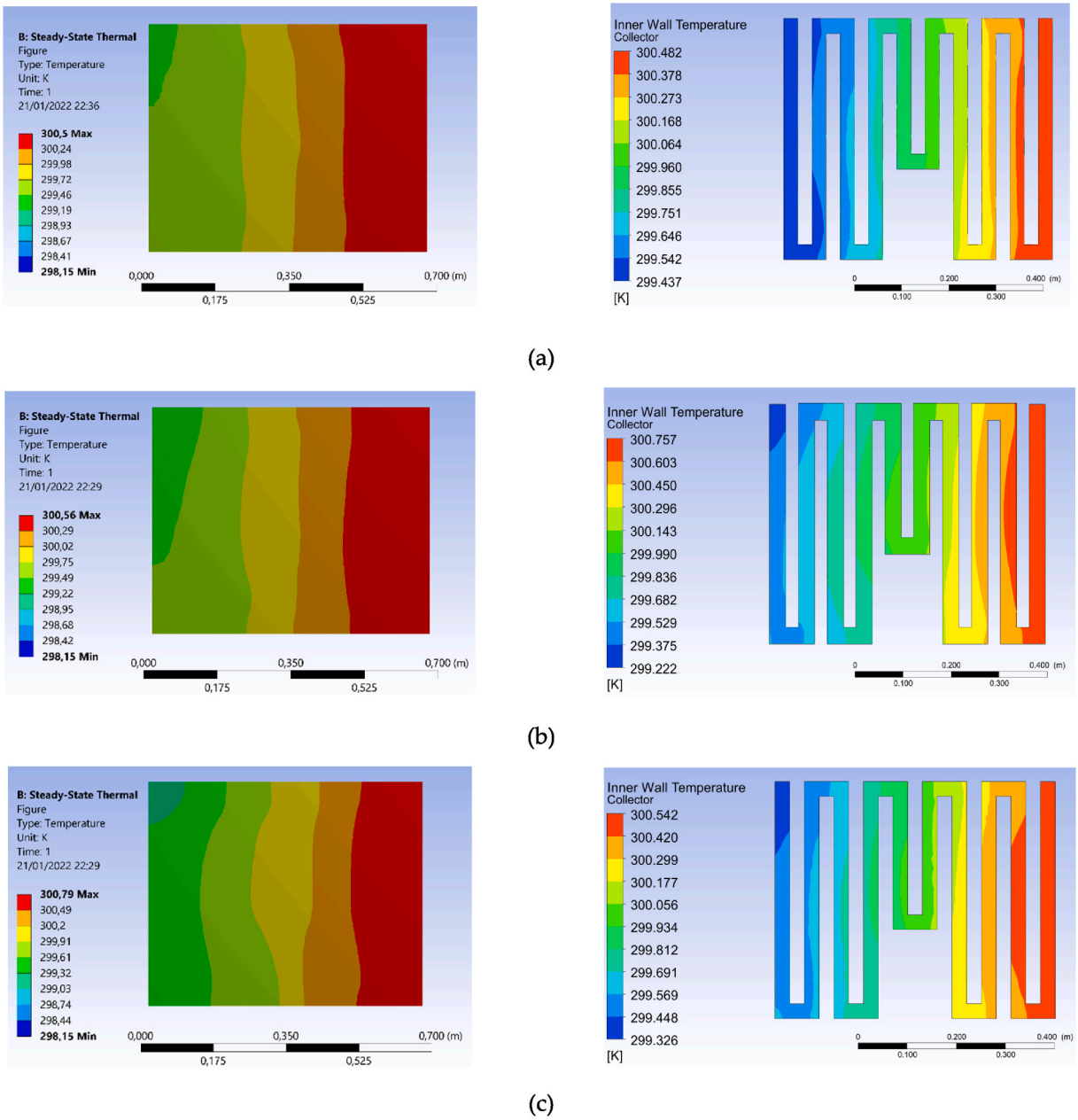

Fig. 14. The contour of PV and collector surfaces in each riser configuration shape: (a) rectangle, (b) triangle, (c) semicircle.

thermal fluid produced is one of the advantages of increasing the performance of photovoltaic solar cells. Improved performance can be observed in the form of thermal efficiency. Thermal efficiency is obtained from the temperature difference at the outlet against the inlet temperature. The temperature difference is multiplied by the mass flow rate and the specific heat capacity of the fluid and divided by the radiation intensity and the collector surface area. Therefore, the difference in fluid temperature specifically dramatically affects the resulting thermal efficiency [85]. As seen in Fig. 20, the highest thermal efficiency of 116% was achieved using the radiation intensity of 600 W/m^2 and water as a fluid. Based on this trend, it can be predicted that the thermal efficiency will decrease as the radiation intensity increases. It can be seen that water s has the highest efficiency value compared to the different nanofluids used in the present study [9]. Using a specific thermal collector system can increase the electrical efficiency and produce thermal efficiency, resulting in binding of solar cell performance.

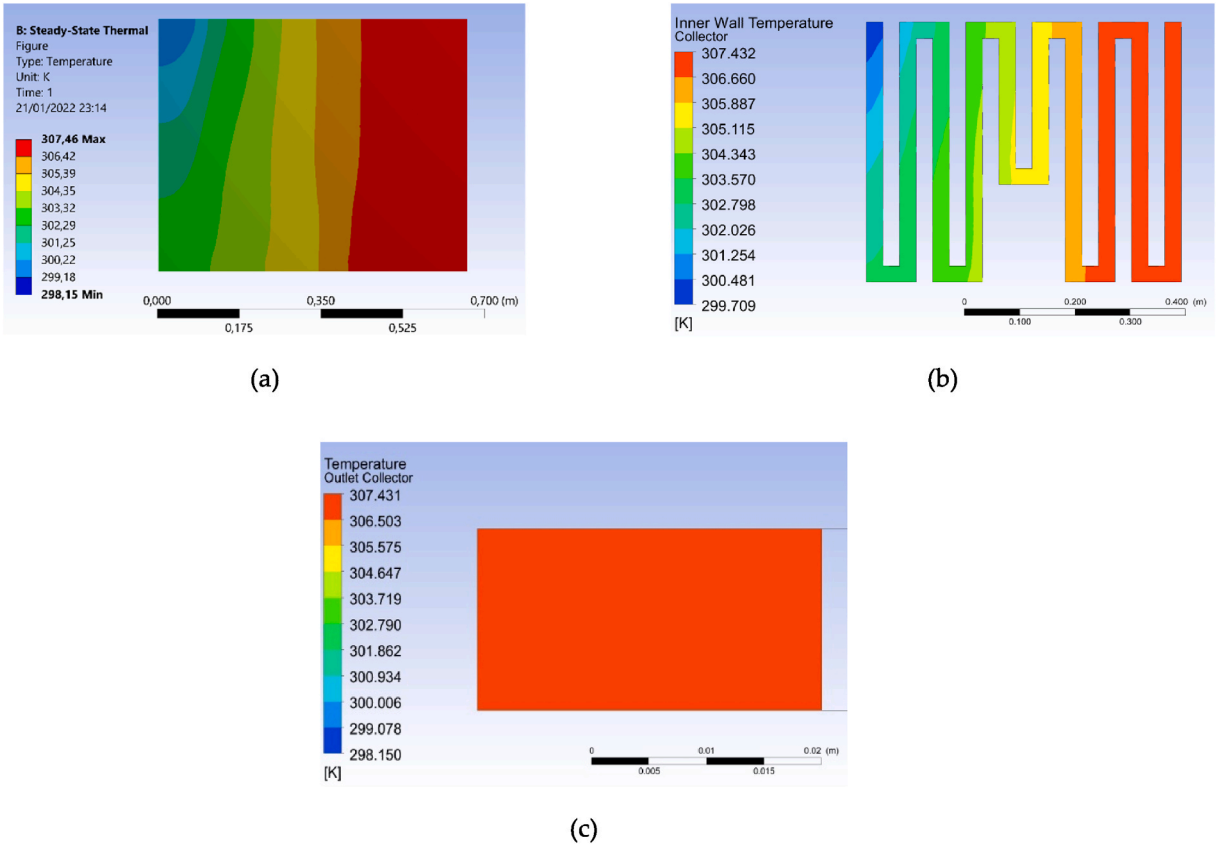

Fig. 15. Temperature contours for (a) PV, (b) collector, and (c) collector outlet in Al_2O_3 working fluid.

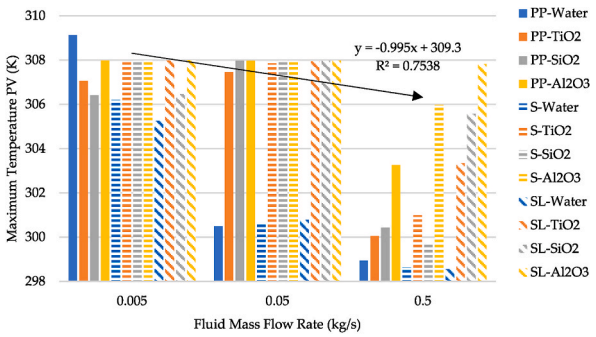

Fig. 16. Effect of the fluid mass flow rate of fluid on maximum temperature PV.

4.5. The efficiency of photovoltaic solar cells in thermal collector systems with different riser collector configuration shapes and fluid types

The electrical and thermal efficiency analysis could be calculated based on the temperature generated during the simulation process using the thermal collector system with different riser collector configurations and fluid types. The differences in the temperature generated for each riser collector configuration shape with the various types of fluids influenced the resulting efficiency. Using the same electrical efficiency analysis process for PV solar cells, it can be determined that there are differences in electrical efficiency even though they are relatively small.

As seen in Fig. 21, using a rectangular collector riser configuration in water resulted in the highest electrical efficiency of 11.87%. Nanofluids have a smaller electrical efficiency value for each riser collector configuration shape [27]. The temperature generated by using the photovoltaic thermal collector system influences the electrical efficiency value. The working fluid flowing through the riser collector configuration depends on its density and viscosity. When the fluid is denser and more viscous, it will affect the flow rate so that the heat transfer time will be slower. In comparison, the heat transfer value is influenced by the specific heat of the working fluid.

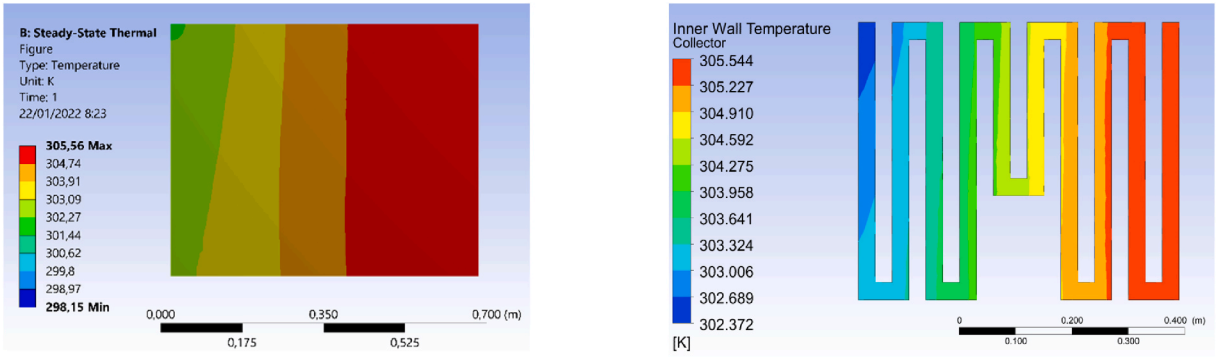

(a)

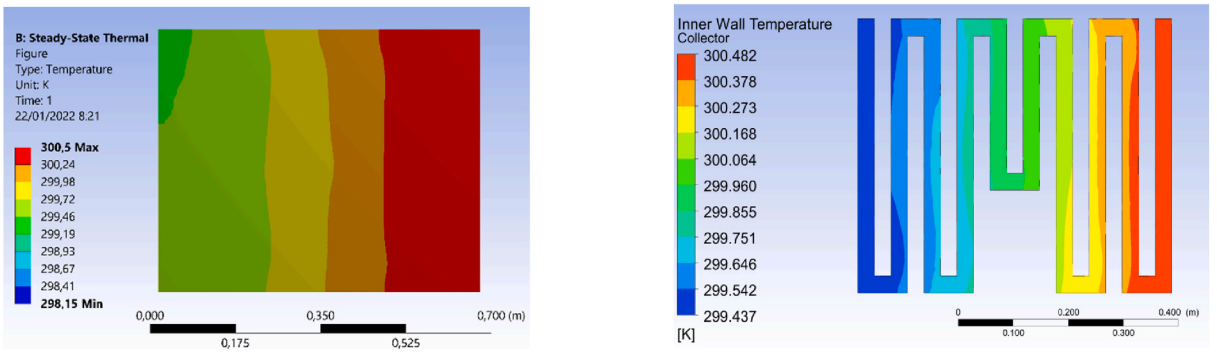

(b)

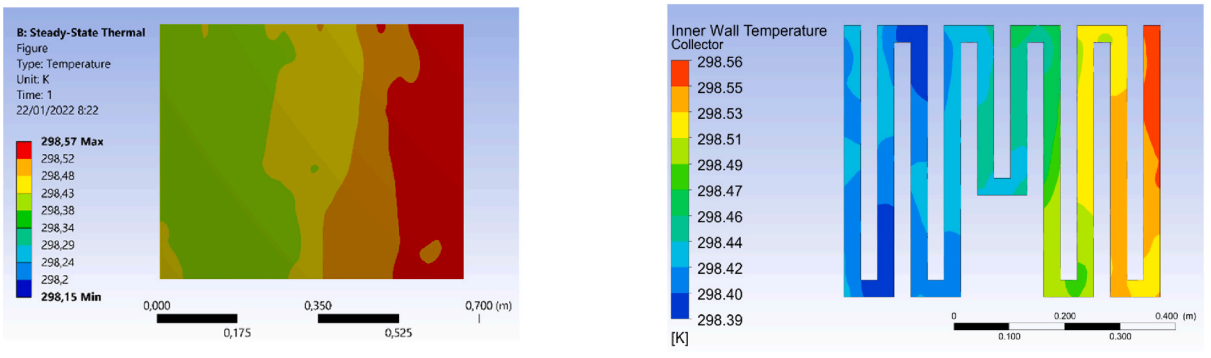

(c)

Fig. 17. PV and collector temperature contours at different mass flow rates: (a) 0.005, (b) 0.05, (c) 0.5 kg/s.

The relatively small differences in the efficiency indicate that the various riser collector configurations do not affect the heat transfer process in the PV solar cells in the collector fluid. This is because the hydraulic value is maintained in the same way, meaning there is not too much difference in heat transfer even though there are differences in shape. The different working fluids used in the riser configuration shape resulted in different electrical efficiencies. Water resulted in a more specific electrical efficiency difference value [88], with the difference in relative efficiency reaching 3.27% due to water having very different fluid characteristics.

Based on the electrical efficiency data generated using the different riser collector shapes, homogeneity tests were carried out using ANOVA analysis to determine the effect. Similar variations were observed in all of the various produced, as shown in Table 9. The results of the ANOVA analysis resulted in a *P*-value of 0.995 with a calculated F of 0.005, as seen in Table 10. The null hypothesis can be accepted because the *P*-value is greater than the predetermined significance value. It can be stated that the shape of the riser collector configuration does not affect the electrical efficiency of the photovoltaic solar cells. The trend char also support this in Fig. 21.

The use of different types of fluids in each riser collector configuration shape affects the efficiency of the electricity generated, as shown in Fig. 21. This is also supported by different variable values in the yield for the working fluid, as shown in Table 11. This results

Table 8
Collector outlet temperature results at each fluid mass flow rate (in K).

Collector Riser Shape	Fluid	Fluid Mass Flow Rate (kg/s)		
		0.005	0.05	0.5
Rectangle	Water	307.005	300.477	298.815
	TiO_2	307.059	307.431	299.991
	SiO_2	306.409	307.968	300.350
	Al_2O_3	307,980	307.971	303.052
Triangle	Water	306.207	300.538	298.607
	TiO_2	307.960	307.849	300.786
	SiO_2	307.973	307.965	299.772
	Al_2O_3	307.982	307.976	305.721
Semicircle	Water	305.244	300.753	298.540
	TiO_2	307.979	307.951	303.081
	SiO_2	306.458	307.967	305.354
	Al_2O_3	307.988	307.979	307.783

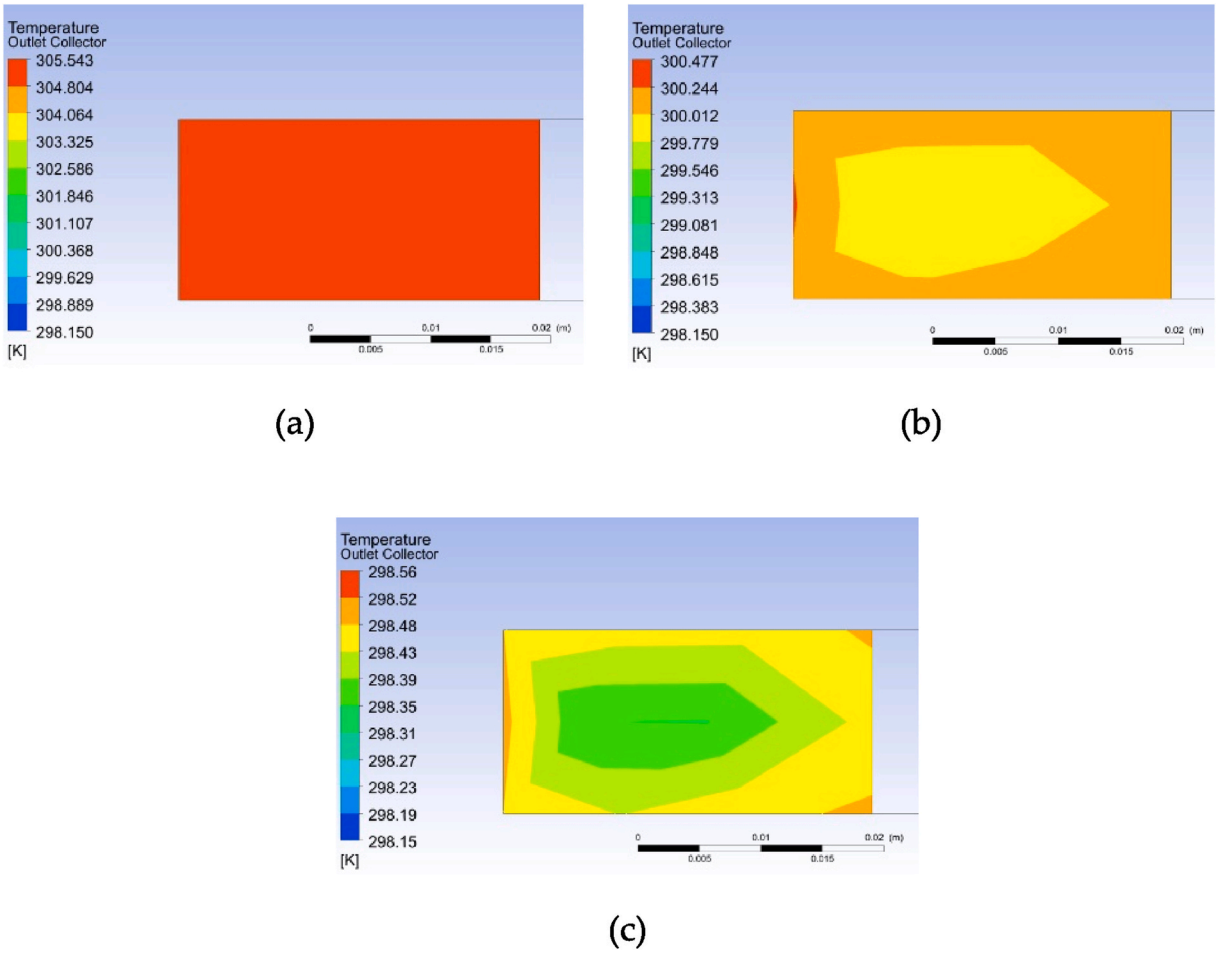

Fig. 18. Temperature distribution contours for the collector outlet at the flow rates of (a) 0.005, (b) 0.05, (c) 0.5 kg/s.

in a *P*-value smaller than 0.05, which is 4 E−08, as shown in Table 12; this means that the null hypothesis should be rejected, supported by a calculated F value that is more significant than the F table. Thus, the working fluid used affects the electrical efficiency of photovoltaic solar cells.

The resulting thermal efficiency can be seen in Fig. 22. Different riser collector configurations demonstrate different trends in the resulting thermal efficiency. Using a semicircular riser collector configuration resulted in high thermal efficiency trends for each working fluid. The semicircular shape allows the fluid to be more compressed, increasing the temperature. The semicircular riser configuration showed the highest thermal efficiency of 121% when water was used as the working fluid. From the research, it can be

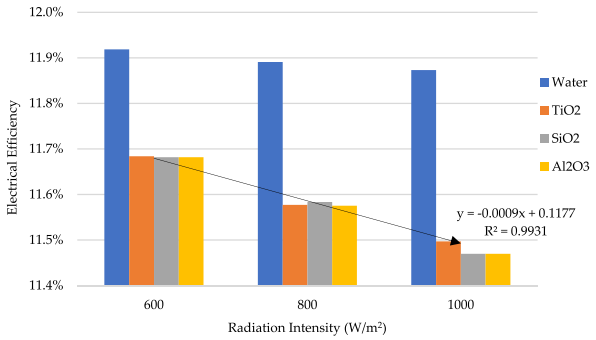

Fig. 19. Effects of radiation intensity on electrical efficiency in photovoltaic thermal collector systems.

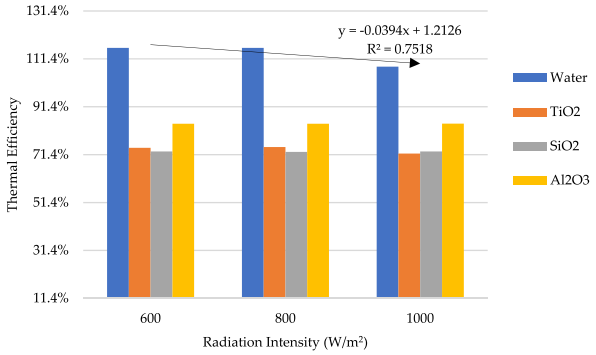

Fig. 20. Effects of radiation intensity on thermal efficiency in photovoltaic thermal collector systems.

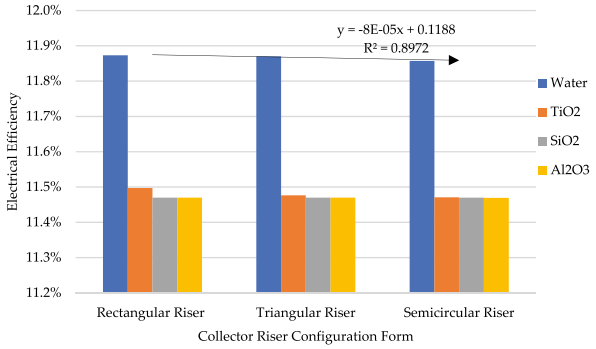

Fig. 21. The influence of riser collector configuration on electrical efficiency in photovoltaic thermal collector systems.

Table 9
Electrical efficiency data for each collector riser configuration shape.

Groups	Count	Sum	Average	Variance
Rectangle	4	0.4623312	0.115583	2.54E-06
Triangle	4	0.462855	0.115714	3.96E-06
Semicircle	4	0.4626714	0.115668	3.75E-06

said that the PVT system with a riser configuration designed based on the input parameters of the fluid flow rate and using nanofluids resulted in the maximum increase in electrical and thermal performance. Nanofluids maximize heat absorption due to increased thermal conductivity and increasing efficiency [89].

Table 10
ANOVA results for the electrical efficiency of each collector riser configuration shape.

Source of Variation	SS	df	MS	F	*P*-value	F crit
Between Groups	3.53E-08	2	1.77E-08	0.005	0.995	4.26
Within Groups	3.08E-05	9	3.42E-06			
Total	3.08E-05	11				

Table 11
Electrical efficiency data for each working fluid.

Groups	Count	Sum	Average	Variance
Water	3	0.355237	0.118412	1.55E-07
TiO_2	3	0.344443	0.114814	1.95E-08
SiO_2	3	0.344092	0.114697	2.89E-34
Al_2O_3	3	0.344086	0.114695	9.72E-12

Table 12
ANOVA results for the electrical efficiency of each working fluid.

Source of Variation	SS	df	MS	F	*P*-value	F crit
Between Groups	3.04E-05	3	1.01E-05	233.20	4E-08	4.07
Within Groups	3.48E-07	8	4.35E-08			
Total	3.08E-05	11				

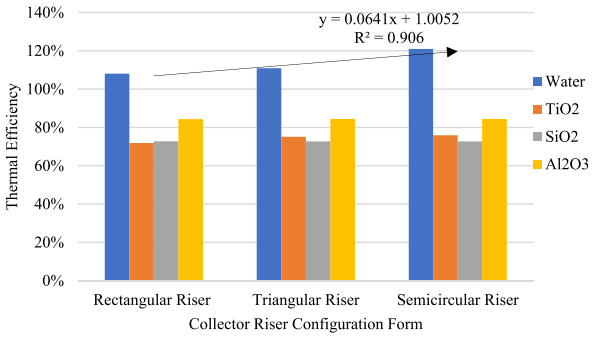

Fig. 22. Effects of riser collector configuration shape on the thermal efficiency of photovoltaic thermal collector systems.

4.6. The efficiency of photovoltaic solar cells in thermal collector systems with different fluid mass flow rates

When using a photovoltaic thermal collector system to cool PV solar cells, the fluid mass flow rate affects the working temperature. Temperature changes due to heat transfer from the solar cells to the working fluid produce electrical and thermal energy. The increase in the performance of PV solar cells can be analyzed based on the electrical and thermal energy produced. The electrical efficiency in

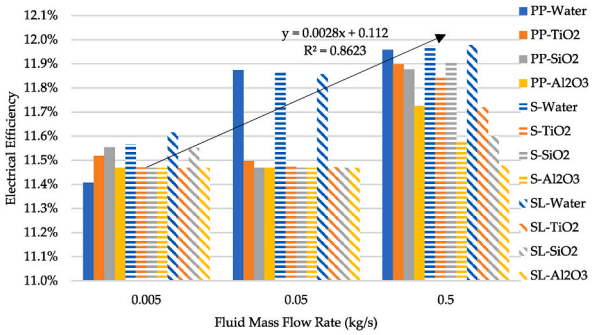

Fig. 23. Effects of the mass fluid flow rate on electrical efficiency in photovoltaic thermal collector systems.

PV solar cells is calculated based on the changes observed in the maximum PV working temperature. In contrast, thermal efficiency is calculated based on fluid inlet and outlet temperatures.

The temperature changes resulting from the simulation process when using a photovoltaic thermal collector system with a radiation intensity of 1000 W/m^2 were successfully carried out. The simulation was conducted by varying the fluid mass flow rate on the different riser collector configurations and fluid types. As seen in Fig. 23, there is a significant difference in the electrical efficiency at the mass flow rate used. Based on the resulting trend, it is known that the efficiency of the electricity generated increases when the fluid mass flow rate increases. Using a semicircular riser configuration with water at a mass flow rate of 0.5 kg/s resulted in the highest electrical efficiency of 11.98%. The high electrical efficiency is due to the significant changes in the maximum PV temperature. When the mass flow rate of the fluid affects the heat transfer that occurs in the PV to the working fluid, the result is a decrease in the temperature of the PV solar cells. Then, the change in the mass flow rate of the fluid affects the efficiency of the electricity generated [76].

The effect of the fluid mass flow rate on the efficiency of the generated electricity was further investigated using ANOVA analysis. In Table 13, the differences in the resulting variations in the electricity efficiency data can be observed. It can be calculated that the calculated F value has a better value than the F table value. The resulting *P*-value of 3.83 E−05 is greater than the specified significance value, as seen in Table 14. Based on this, the null hypothesis is rejected. It can be said that the mass flow rate affects the electrical efficiency of photovoltaic solar cells.

The maximum temperature change in PV solar cells also results in a significant temperature difference in the working fluid. The difference between the working fluid at the outlet and the inlet results in better thermal efficiency. As in Fig. 24, the resulting thermal efficiency trend increases as the fluid mass flow rate increases. It was determined that using a mass flow rate of 0.5 kg/s with an Al_2O_3 working fluid in a semicircular riser collector configuration resulted in the highest thermal efficiency of 827%. The increased temperature and the fluid mass flow rate used are responsible for this result [19].

5. Conclusions

A photovoltaic thermal collector system in a solar cell cooling system was modeled successfully. A simulation process investigated the thermal collector cooling system that was developed. Simulations were carried out using ANSYS software with steady-state thermal modeling on photovoltaic solar cells and fluent modeling on the collector fluids. The modeling was carried out in a coupled manner to determine the temperature changes in the PV solar cells and the collector fluid. As such, it was determined that the photovoltaic thermal collector system could improve the performance of photovoltaic solar cells. It increases the electrical efficiency of photovoltaic solar cells and calculates the thermal efficiency.

Improving the performance of photovoltaic solar cells was carried out by using a photovoltaic thermal collector system. A photovoltaic thermal collector system was used by varying the radiation intensity, the shape of the collector design, the type of fluid, and the fluid flow rate to determine the system's electrical efficiency and thermal efficiency. The simulation process produced temperature distribution and contours on the PV solar cells and working fluid that allowed the efficiency achieved by increasing the performance of photovoltaic solar cells to be calculated.

Based on this research, the rectangular riser collector configuration with water demonstrated the highest electrical efficiency of 11.87%. The semicircular riser con-figuration with water demonstrated the highest thermal efficiency of 121%. Using a riser collector configuration to cool photovoltaic solar cells via a photovoltaic thermal collector system did not affect the electrical efficiency of photovoltaic solar cells. The working fluid used for each riser collector configuration shape affected the electrical efficiency of the photovoltaic solar cells. The use of water resulted in a higher efficiency than any of the nanofluids that were tested, achieving efficiencies up to 3.27% higher. When using a fluid mass flow rate of 0.5 kg/s in each riser collector configuration and type of fluid, significant electrical efficiencies were achieved for the photovoltaic solar cells, with the highest efficiency being 11.98%. For comparison, the resulting thermal efficiency was 82.7%. As such, the mass flow rate of the working fluid in different riser collector configurations can affect the electrical efficiency of photovoltaic solar cells.

Author contribution statement

Singgih Dwi Prasetyo: Conceived and designed the experiments; Performed the experiments; Analyzed and interpreted the data; Wrote the paper.

Aditya Rio Prabowo: Conceived and designed the experiments; Analyzed and interpreted the data; Contributed reagents, materials, analysis tools or data; Wrote the paper.

Zainal Arifin: Conceived and designed the experiments; Performed the experiments; Analyzed and interpreted the data; Contributed reagents, materials, analysis tools or data.

Table 13
Electrical efficiency data for each fluid mass flow rate.

Groups	Count	Sum	Average	Variance
0.5	12	1.415425	0.117952	294.0E-06
0.05	12	1.387858	0.115655	2.8E-06
0.005	12	1.380281	0.115023	0.34E-06

Table 14
ANOVA results for the electrical efficiency of each fluid mass flow rate.

Source of Variation	SS	df	MS	F	*P*-value	F crit
Between Groups	5.7E-05	2	2.85E-05	14.06	3.83E-05	3.28
Within Groups	6.69E-05	33	2.03E-06			
Total	0.000124	35				

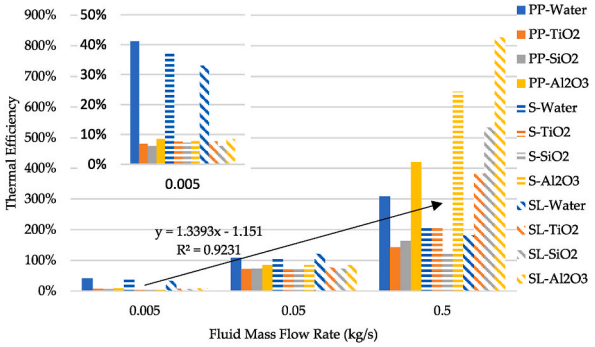

Fig. 24. Effects of the mass flow rate on thermal efficiency in photovoltaic thermal collector systems.

Funding statement

This research was fully supported by a PNBP grant from the Universitas Sebelas Maret, Indonesia, with title "Pengembangan Thermal Collector System Dengan Fluida Nano Untuk Mening-katkan Unjuk Kerja Photovoltaic" scheme PUT 2022 Contract No. 254/UN27.22/PT.01.03/202.

Data availability statement

Data included in article/supp. material/referenced in article.

Declaration of interest's statement

The authors declare no competing interests.

References

[1] F. Afshari, A. Sözen, A. Khanlari, A.D. Tuncer, C. Şirin, Effect of turbulator modifications on the thermal performance of cost-effective alternative solar air heater, Renew. Energy 158 (2020) 297–310, https://doi.org/10.1016/j.renene.2020.05.148.
[2] M. Dang, Solar energy potential in Indonesia, 19Th Int. Conf. Young Sci. 199 (2017).
[3] S.D. Prasetyo, C. Harsito, Sutanto, Suyitno Energy consumption of spray dryer machine for producing red natural powder dye and its stability, AIP Conf. Proc. 2097 (2019) 1–7, https://doi.org/10.1063/1.5098251.
[4] A.D. Tuncer, A. Sözen, F. Afshari, A. Khanlari, C. Şirin, A. Gungor, Testing of a novel convex-type solar absorber drying chamber in dehumidification process of municipal sewage sludge, J. Clean. Prod. (2020) 272, https://doi.org/10.1016/j.jclepro.2020.122862.
[5] Hardianto utilization of solar power plant in Indonesia: a review, Int. J. Environ. Eng. Educ. 1 (2019) 1–8, https://doi.org/10.55151/ijeedu.
[6] T. Saga, Advances in crystalline silicon solar cell technology for industrial mass production, NPG Asia Mater. 2 (2010) 96–102.
[7] M. Azadi, A.S. Rouhaghdam, S. Ahangarani, A review on titanium nitride and titanium carbide single and multilayer coatings deposited by plasma assisted chemical vapor deposition, Int. J. Eng. 29 (2016) 677–687, https://doi.org/10.5829/idosi.ije.2016.29.05b.12.
[8] L.L. Tobin, T. O'Reilly, D. Zerulla, J.T. Sheridan, Characterising dye-sensitised solar cells, Optik 122 (2011) 1225–1230, https://doi.org/10.1016/j.ijleo.2010.07.028.
[9] M. Chandrasekar, S. Suresh, T. Senthilkumar, M. Ganesh Karthikeyan, Passive cooling of standalone flat PV module with cotton wick structures, Energy Convers. Manag. 71 (2013) 43–50, https://doi.org/10.1016/j.enconman.2013.03.012.
[10] H. Ramdani, C. Ould-Lahoucine, Study on the overall energy and exergy performances of a novel water-based hybrid photovoltaic-thermal solar collector, Energy Convers. Manag. 222 (2020), 113238, https://doi.org/10.1016/j.enconman.2020.113238.
[11] S. Wu, C. Xiong, Passive cooling technology for photovoltaic panels for domestic houses, Int. J. Low Carbon Technol. 9 (2014) 118–126, https://doi.org/10.1093/ijlct/ctu013.
[12] G. Setyohandoko, B. Sutanto, R.A. Rachmanto, D.D. Dwi Prija Tjahjana, Z. Arifin, A numerical approach to study the performance of photovoltaic panels by using aluminium heat sink, J. Adv. Res. Fluid Mech. Therm. Sci. 70 (2020) 97–105, https://doi.org/10.37934/ARFMTS.70.2.97105.
[13] H.G. Teo, P.S. Lee, M.N.A. Hawlader, An active cooling system for photovoltaic modules, Appl. Energy 90 (2012) 309–315, https://doi.org/10.1016/j.apenergy.2011.01.017.
[14] D. Sato, N. Yamada, Review of photovoltaic module cooling methods and performance evaluation of the radiative cooling method, Renew. Sustain. Energy Rev. 104 (2019) 151–166, https://doi.org/10.1016/j.rser.2018.12.051.
[15] S.D. Prasetyo, A.R. Prabowo, Z. Arifin, The effect of collector design in increasing PVT performance: current state and milestone, Mater. Today Proc. (2022), https://doi.org/10.1016/j.matpr.2021.12.356.

[16] H.A. Kazem, M.T. Chaichan, A.H.A. Al-Waeli, K. Sopian, Comparison and evaluation of solar photovoltaic thermal system with hybrid collector: an experimental study, Therm. Sci. Eng. Prog. 22 (2021), 100845, https://doi.org/10.1016/j.tsep.2021.100845.
[17] M. Teymori-omran, A. Motevali, S. Reza Mousavi Seyedi, M. Montazeri, Numerical simulation and experimental validation of a photovoltaic/thermal system: performance comparison inside and outside greenhouse, Sustain. Energy Technol. Assessments 46 (2021), 101271, https://doi.org/10.1016/j.seta.2021.101271.
[18] A.H.A. Al-Waeli, K. Sopian, M.T. Chaichan, H.A. Kazem, H.A. Hasan, A.N. Al-Shamani, An experimental investigation of SiC nanofluid as a base-fluid for a photovoltaic thermal PV/T system, Energy Convers. Manag. 142 (2017) 547–558, https://doi.org/10.1016/j.enconman.2017.03.076.
[19] A. Abadeh, O. Rejeb, M. Sardarabadi, C. Menezo, M. Passandideh-Fard, A. Jemni, Economic and environmental analysis of using metal-oxides/water nanofluid in photovoltaic thermal systems (PVTs), Energy 159 (2018) 1234–1243, https://doi.org/10.1016/j.energy.2018.06.089.
[20] S.R. Abdallah, I.M.M. Elsemary, A.A. Altohamy, M.A. Abdelrahman, A.A.A. Attia, O.E. Abdellatif, Experimental investigation on the effect of using nano fluid (Al2O3-Water) on the performance of PV/T system, Therm. Sci. Eng. Prog. 7 (2018) 1–7, https://doi.org/10.1016/j.tsep.2018.04.016.
[21] M.M. Sardouei, H. Mortezapour, K. Jafari Naeimi, Temperature distribution and efficiency assessment of different PVT water collector designs, Sadhana - Acad. Proc. Eng. Sci. 43 (2018), https://doi.org/10.1007/s12046-018-0826-x.
[22] J.-S. Yu, J.-H. Kim, J.-T. Kim, Effect of triangular baffle arrangement on heat transfer enhancement of air-type PVT collector, Sustain. Times 12 (2020), https://doi.org/10.3390/SU12187469.
[23] S. Misha, A.L. Abdullah, N. Tamaldin, M.A.M. Rosli, F.A. Sachit, Simulation CFD and experimental investigation of PVT water system under natural Malaysian weather conditions, Energy Rep. 6 (2020) 28–44, https://doi.org/10.1016/j.egyr.2019.11.162.
[24] S. Peng, Y. Kon, H. Watanabe, Effects of sea breeze on urban areas using computation fluid dynamic—a case study of the range of cooling and humidity effects in sendai, Japan, Sustain. Times 14 (2022), https://doi.org/10.3390/su14031074.
[25] A.N. Al-Shamani, M.A. Alghoul, A.M. Elbreki, A.A. Ammar, A.M. Abed, K. Sopian, Mathematical and experimental evaluation of thermal and electrical efficiency of PV/T collector using different water based nano-fluids, Energy 145 (2018) 770–792, https://doi.org/10.1016/j.energy.2017.11.156.
[26] M.A.M. Rosli, Y.J. Ping, S. Misha, M.Z. Akop, K. Sopian, S. Mat, A.N. Al-Shamani, M.A. Saruni, Simulation study of computational fluid dynamics on photovoltaic thermal water collector with different designs of absorber tube, J. Adv. Res. Fluid Mech. Therm. Sci. 52 (2018) 12–22.
[27] M. Herrando, A. Ramos, I. Zabalza, C.N. Markides, A comprehensive assessment of alternative absorber-exchanger designs for hybrid PVT-water collectors, Appl. Energy 235 (2019) 1583–1602, https://doi.org/10.1016/j.apenergy.2018.11.024.
[28] Z. Arifin, S.D. Prasetyo, A.R. Prabowo, D.D.D.P. Tjahjana, R.A. Rachmanto, Effect of thermal collector configuration on the photovoltaic heat transfer performance with 3D CFD modeling, Open Eng. 11 (2021) 1076–1085, https://doi.org/10.1515/eng-2021-0107.
[29] A. Khanlari, A. Sözen, F. Afshari, A.D. Tuncer, Energy-exergy and sustainability analysis of a PV-driven quadruple-flow solar drying system, Renew. Energy 175 (2021) 1151–1166, https://doi.org/10.1016/j.renene.2021.05.062.
[30] E. Çiftçi, A. Khanlari, A. Sözen, İ. Aytaç, A.D. Tuncer, Energy and exergy analysis of a photovoltaic thermal (PVT) system used in solar dryer: a numerical and experimental investigation, Renew. Energy 180 (2021) 410–423, https://doi.org/10.1016/j.renene.2021.08.081.
[31] N.K. Baranwal, M.K. Singhal, Modeling and simulation of a spiral type hybrid photovoltaic thermal (PV/T) water collector using ANSYS, in: Advances in Clean Energy Technologies, Springer, Singapore, 2021, pp. 127–139.
[32] B. Eisavi, H. Nami, M. Yari, F. Ranjbar, Solar-driven mechanical vapor compression desalination equipped with organic Rankine cycle to supply domestic distilled water and power – thermodynamic and exergoeconomic implications, Appl. Therm. Eng. 193 (2021), 116997, https://doi.org/10.1016/j.applthermaleng.2021.116997.
[33] M. Rahimi, A. Joudavi, Solar Energy Potential in Serbia, 2020.
[34] S. Rühle, M. Shalom, A. Zaban, Quantum-dot-sensitized solar cells, ChemPhysChem 11 (2010) 2290–2304, https://doi.org/10.1002/cphc.201000069.
[35] I. Guarracino, A. Mellor, N.J. Ekins-Daukes, C.N. Markides, Dynamic coupled thermal-and-electrical modelling of sheet-and-tube hybrid photovoltaic/thermal (PVT) collectors, Appl. Therm. Eng. 101 (2016) 778–795, https://doi.org/10.1016/j.applthermaleng.2016.02.056.
[36] A.N. Al-Shamani, K. Sopian, S. Mat, A.M. Abed, Performance enhancement of photovoltaic grid-connected system using PVT panels with nanofluid, Sol. Energy 150 (2017) 38–48, https://doi.org/10.1016/j.solener.2017.04.005.
[37] M. Dannemand, B. Perers, S. Furbo, Performance of a demonstration solar PVT assisted heat pump system with cold buffer storage and domestic hot water storage tanks, Energy Build. 188–189 (2019) 46–57, https://doi.org/10.1016/j.enbuild.2018.12.042.
[38] A. Zabihi Sheshpoli, O. Jahanian, K. Nikzadfar, M. Aghajani Delavar, Numerical and experimental investigation on the performance of hybrid PV/thermal systems in the north of Iran, Sol. Energy 215 (2021) 108–120, https://doi.org/10.1016/j.solener.2020.12.036.
[39] B. Widyolar, L. Jiang, J. Ferry, R. Winston, A. Kirk, M. Osowski, D. Cygan, H. Abbasi, Theoretical and experimental performance of a two-stage (50X) hybrid spectrum splitting solar collector tested to 600 °C, Appl. Energy 239 (2019) 514–525, https://doi.org/10.1016/j.apenergy.2019.01.172.
[40] W. He, T.T. Chow, J. Ji, J. Lu, G. Pei, L.S. Chan, Hybrid photovoltaic and thermal solar-collector designed for natural circulation of water, Appl. Energy 83 (2006) 199–210, https://doi.org/10.1016/j.apenergy.2005.02.007.
[41] N. Aste, C. del Pero, F. Leonforte, Water flat plate PV-thermal collectors: a review, Sol. Energy 102 (2014) 98–115, https://doi.org/10.1016/j.solener.2014.01.025.
[42] A. Adel, Hegazy Comparative study of the performances of four photovoltaic/thermal solar air collectors, Energy Convers. Manag. 41 (2000) 861–881.
[43] J.K. Tonui, Y. Tripanagnostopoulos, Air-cooled PV/T solar collectors with low cost performance improvements, Sol. Energy 81 (2007) 498–511.
[44] S. Tiwari, S. Agrawal, G.N. Tiwari, PVT air collector integrated greenhouse dryers, Renew. Sustain. Energy Rev. 90 (2018) 142–159.
[45] A. Gaur, G.N. Tiwari, C. Ménézo, I.M. Al-Helal, Numerical and experimental studies on a Building integrated Semi-transparent Photovoltaic Thermal (BiSPVT) system: model validation with a prototype test setup, Energy Convers. Manag. 129 (2016) 329–343.
[46] C.J. Ho, W.L. Chou, C.M. Lai, Thermal and electrical performance of a water-surface floating PV integrated with a water-saturated MEPCM layer, Energy Convers. Manag. 89 (2015) 862–872, https://doi.org/10.1016/j.enconman.2014.10.039.
[47] A.C. Beath, Industrial energy usage in Australia and the potential for implementation of solar thermal heat and power, Energy 43 (2012) 261–272, https://doi.org/10.1016/j.energy.2012.04.031.
[48] J.S. Coventry, K. Lovegrove, Development of an approach to compare the 'value' of electrical and thermal output from a domestic PV/thermal system, Sol. Energy 75 (2003) 63–72, https://doi.org/10.1016/S0038-092X(03)00231-7.
[49] T.T. Chow, W. He, J. Ji, An experimental study of façade-integrated photovoltaic/water-heating system, Appl. Therm. Eng. 27 (2007) 37–45, https://doi.org/10.1016/j.applthermaleng.2006.05.015.
[50] G. Singh, S. Kumar, G.N. Tiwari, Design, fabrication and performance evaluation of a hybrid photovoltaic thermal (PVT) double slope active solar still, Desalination 277 (2011) 399–406, https://doi.org/10.1016/j.desal.2011.04.064.
[51] L.C. Kelley, S. Dubowsky, Thermal control to maximize photovoltaic powered reverse osmosis desalination systems productivity, Desalination 314 (2013) 10–19, https://doi.org/10.1016/j.desal.2012.11.036.
[52] Y. Jia, G. Alva, G. Fang, Development and applications of photovoltaic–thermal systems: a review, Renew. Sustain. Energy Rev. 102 (2019) 249–265.
[53] E.K. Akpinar, Drying of mint leaves in a solar dryer and under open sun: modelling, performance analyses, Energy Convers. Manag. 51 (2010) 2407–2418, https://doi.org/10.1016/j.enconman.2010.05.005.
[54] D.B. Singh, J.K. Yadav, V.K. Dwivedi, S. Kumar, G.N. Tiwari, I.M. Al-Helal, Experimental studies of active solar still integrated with two hybrid PVT collectors, Sol. Energy 130 (2016) 207–223, https://doi.org/10.1016/j.solener.2016.02.024.
[55] A. Alaudeen, K. Johnson, P. Ganasundar, A. Syed Abuthahir, K. Srithar, Study on stepped type basin in a solar still, J. King Saud Univ. - Eng. Sci. 26 (2014) 176–183, https://doi.org/10.1016/j.jksues.2013.05.002.
[56] I. Alphonse, S. Hosiminthilagar, F. Bright Singh, Design of Solar Powered BLDC Motor Driven Electric Vehicle, vol. 2, 2012.
[57] A.K. Digalwar, G. Giridhar, Interpretive Structural modeling approach for development of Electric Vehicle market in India, Procedia CIRP 26 (2015) 40–45, https://doi.org/10.1016/j.procir.2014.07.125.

[58] M. Grandone, M. Naddeo, D. Marra, G. Rizzo, Development of a regenerative braking control strategy for hybridized solar vehicle, in: Proceedings of the IFAC-PapersOnLine, vol. 49, Elsevier B.V., 2016, pp. 497–504.
[59] F. Kineavy, M. Duffy, Modelling and Design of Electric Vehicle Charging Systems that Include On-Site Renewable Energy Sources, 2014, ISBN 978-1-4799-5115-4.
[60] R.U. Khan, B. Bhattacharyya, G. Singh, Experimental study of modified dual slope hybrid photovoltaic (PV/T) solar thermal still, Desalination Water Treat. 156 (2019) 168–176, https://doi.org/10.5004/dwt.2019.24113.
[61] M. Waseem, A.F. Sherwani, M. Suhaib, Integration of solar energy in electrical, hybrid, autonomous vehicles: a technological review, SN Appl. Sci. 1 (2019) 1–14, https://doi.org/10.1007/s42452-019-1458-4.
[62] U. Eicker, A. Colmenar-Santos, L. Teran, M. Cotrado, D. Borge-Diez, Economic evaluation of solar thermal and photovoltaic cooling systems through simulation in different climatic conditions: an analysis in three different cities in Europe, Energy Build. 70 (2014) 207–223, https://doi.org/10.1016/j.enbuild.2013.11.061.
[63] Y.B. Assoa, C. Ménézo, G. Fraisse, R. Yezou, J. Brau, Study of a new concept of PhotoVoltaic-Thermal hybrid collector, Sol. Energy 81 (2007) 1132–1143, https://doi.org/10.1016/j.solener.2007.04.001.
[64] S. Dubey, G.S. Sandhu, G. Tiwari, Analytical expression for electrical efficiency of PV/T hybrid air collector, Appl. Energy 86 (2009) 697–705.
[65] Y. Tripanagnostopoulos, M. Souliotis, P. Yianoulis, T.N. Hybrid photovoltaic/thermal solar systems, Sol. Energy 72 (2002) 217–234.
[66] G. Hailu, P. Dash, A.S. Fung, Performance evaluation of an air source heat pump coupled with a building-integrated photovoltaic/thermal (BIPV/T) System under cold climatic conditions, in: Proceedings of the Energy Procedia, vol. 78, Elsevier Ltd, 2015, pp. 1913–1918.
[67] V. Michalcová, K. Kotrasová, The numerical diffusion effect on the cfd simulation accuracy of velocity and temperature field for the application of sustainable architecture methodology, Sustain. Times 12 (2020) 1–18, https://doi.org/10.3390/su122310173.
[68] C.G. Popovici, S.V. Hudişteanu, T.D. Mateescu, N.C. Cherecheş, Efficiency improvement of photovoltaic panels by using air cooled heat sinks, Proceedings of the Energy Procedia 85 (2016) 425–432.
[69] A.F. Fadli, B. Kristiawan, Suyitno, Z. Arifin, Analysis of TiO 2/Water-based photovoltaic thermal (PV/T) collector to improve solar cell performance, IOP Conf. Ser. Mater. Sci. Eng. 1096 (2021), 012053, https://doi.org/10.1088/1757-899x/1096/1/012053.
[70] B. Sutanto, Simulation and Experiment of Cooling System for Floating Photovoltaic Module with Thermosiphon Method, 2018, p. 23116301.
[71] A.N. Al-Shamani, K. Sopian, S. Mat, H.A. Hasan, A.M. Abed, M.H. Ruslan, Experimental studies of rectangular tube absorber photovoltaic thermal collector with various types of nanofluids under the tropical climate conditions, Energy Convers. Manag. 124 (2016) 528–542, https://doi.org/10.1016/j.enconman.2016.07.052.
[72] H. Xie, W. Yu, W. Chen, MgO nanofluids: higher thermal conductivity and lower viscosity among ethylene glycol-based nanofluids containing oxide nanoparticles, J. Exp. Nanosci. 5 (2010) 463–472, https://doi.org/10.1080/17458081003628949.
[73] Z. Arifin, D.D.D.P. Tjahjana, S. Hadi, R.A. Rachmanto, G. Setyohandoko, B. Sutanto, Numerical and experimental investigation of air cooling for photovoltaic panels using aluminum heat sinks, Int. J. Photoenergy 2020 (2020) 1–9, https://doi.org/10.1155/2020/1574274.
[74] S. Abdo, H. Saidani-Scott, M.A. Abdelrahman, Numerical study with eco-exergy analysis and sustainability assessment for a stand-alone nanofluid PV/T, Therm. Sci. Eng. Prog. 24 (2021), 100931, https://doi.org/10.1016/j.tsep.2021.100931.
[75] H. Khoshvaght, M. Delnavaz, M. Leili, Optimization of acetaminophen removal from high load synthetic pharmaceutical wastewater by experimental and ANOVA analysis, J. Water Proc. Eng. 42 (2021), 102107, https://doi.org/10.1016/j.jwpe.2021.102107.
[76] M.A. Arefin, M.T. Islam, M. Zunaed, K. Mostakim, Performance analysis of a novel integrated photovoltaic-thermal system by top-surface forced circulation of water, Clean Energy 4 (2020) 316–327, https://doi.org/10.1093/ce/zkaa018.
[77] F. Calise, R.D. Figaj, L. Vanoli, Experimental and numerical analyses of a flat plate photovoltaic/thermal solar collector, Energies 10 (2017), https://doi.org/10.3390/en10040491.
[78] M. Mustapha, A. Fudholi, K. Sopian, Mathematical modelling of bifacial photovoltaic-thermal (BPVT) collector with mirror reflector, Int. J. Renew. Energy Resour. 10 (2020) 654–662, https://doi.org/10.20508/ijrer.v10i2.10603.g7936.
[79] S. Brötje, M. Kirchner, F. Giovannetti, Performance and heat transfer analysis of uncovered photovoltaic-thermal collectors with detachable compound, Sol. Energy 170 (2018) 406–418, https://doi.org/10.1016/j.solener.2018.05.030.
[80] W. Pang, B.C. Duck, C.J. Fell, G.J. Wilson, W. Zhao, H. Yan, Influence of multiple factors on performance of photovoltaic-thermal modules, Sol. Energy 214 (2021) 642–654, https://doi.org/10.1016/j.solener.2020.11.050.
[81] F. Calise, R.D. Figaj, L. Vanoli, Energy performance of a low-cost PhotoVoltaic/Thermal (PVT) collector with and without thermal insulation, in: Proceedings of the IOP Conference Series: Earth and Environmental Science, vol. 214, 2019.
[82] H.A. Kazem, A.H.A. Al-Waeli, M.T. Chaichan, K.H. Al-Waeli, A.B. Al-Aasam, K. Sopian, Evaluation and comparison of different flow configurations PVT systems in Oman: a numerical and experimental investigation, Sol. Energy 208 (2020) 58–88, https://doi.org/10.1016/j.solener.2020.07.078.
[83] S.M. Bambrook, A.B. Sproul, Maximising the energy output of a PVT air system, Sol. Energy 86 (2012) 1857–1871, https://doi.org/10.1016/j.solener.2012.02.038.
[84] M. Lämmle, M. Hermann, K. Kramer, C. Panzer, A. Piekarczyk, C. Thoma, S. Fahr, Development of highly efficient, glazed PVT collectors with overheating protection to increase reliability and enhance energy yields, Sol. Energy 176 (2018) 87–97, https://doi.org/10.1016/j.solener.2018.09.082.
[85] M.O. Lari, A.Z. Sahin, Design, performance and economic analysis of a nanofluid-based photovoltaic/thermal system for residential applications, Energy Convers. Manag. 149 (2017) 467–484, https://doi.org/10.1016/j.enconman.2017.07.045.
[86] M. Modrek, A. Al-Alili, Thermal and electrical performance of a flat plate photovoltaic/thermal collector, in: Proceedings of the ASME 2017 11th International Conference on Energy Sustainability, American Society of Mechanical Engineers, 2017.
[87] M. Herrando, A. Ramos, J. Freeman, I. Zabalza, C.N. Markides, Technoeconomic modelling and optimisation of solar combined heat and power systems based on flat-box PVT collectors for domestic applications, Energy Convers. Manag. 175 (2018) 67–85, https://doi.org/10.1016/j.enconman.2018.07.045.
[88] E. Bellos, C. Tzivanidis, N. Nikolaou, Investigation and optimization of a solar assisted heat pump driven by nanofluid-based hybrid PV, Energy Convers. Manag. (2019) 198, https://doi.org/10.1016/j.enconman.2019.111831.
[89] G.S. Menon, S. Murali, J. Elias, D.S. Aniesrani Delfiya, P.V. Alfiya, M.P. Samuel, Experimental investigations on unglazed photovoltaic-thermal (PVT) system using water and nanofluid cooling medium, Renew. Energy (2022) 188, https://doi.org/10.1016/j.renene.2022.02.080.